Journal of Integrative Neuroscience

J. Integr. Neurosci. **2026**; 25(8): 52511
https://doi.org/10.31083/JIN52511

Review

Controlling the Triple Network Model: Salience Network Modulatory Roles, Default Mode Dynamic Functions, and Central Executive Network Heterogeneity

Martin Pham[1], Sonia Odutola[2], Hrishikesh Pable[2], Robin Chhabra[3], Amedeo D'Angiulli[2,*]

[1]Department of Computer Science, University of Toronto, Toronto, ON M5S 2E4, Canada
[2]Department of Neuroscience, Carleton University, Ottawa, ON K1S 5B6, Canada
[3]Department of Mechanical, Industrial and Mechatronics Engineering, Toronto Metropolitan University, Toronto, ON M5B 2K3, Canada
*Correspondence: amedeo.dangiulli@carleton.ca (Amedeo D'Angiulli)
Academic Editor: Bettina Platt
Submitted: 1 April 2026 Revised: 24 May 2026 Accepted: 10 June 2026 Published: 26 August 2026

Abstract

The triple network model has become a widely adopted framework for studying large-scale brain organization in basic and clinical neuroscience; however, accumulating evidence complicates this taxonomy. The default mode network, once labelled "task-negative", is now recognized as dynamically engaged across both internally directed and task-related processes. The salience network, often described as a "switching" hub, exerts context-dependent modulatory influences on both default mode and central executive network activity, supported by oscillatory coupling and directed connectivity. The central executive and frontoparietal networks, traditionally viewed as a unitary task-positive network, display heterogeneity across parcellations and frequency bands, suggesting finer-grained functional subdivisions than previously assumed. Multimodal studies integrating electroencephalography, functional magnetic resonance imaging, and other approaches converge on the view that networks interact through flexible, frequency-specific dynamics, but diverge in their anatomical assignments depending on atlas, modality, and task. In this scoping review synthesizes evidence on network definitions, methodological inconsistencies, and putative modulatory mechanisms, highlighting the heterogeneity of control networks and underscoring the need to incorporate temporal dynamics into future taxonomies. We propose that geometric hypotheses of neural control describing the global coordination of local activities, such as those used in neural manifolds, may improve our understanding of disordered cognition by integrating the many existing methodologically constrained maps into a coherent stable atlas that is more robust to approximating biases and errors associated with sampled population variability.

Keywords: brain mapping; signal processing; default mode network

1. Introduction

The triple network model (3NM) proposes a system with three major networks—the Default Mode Network (DMN), the Salience Network (SN), and the Central Executive Network (CEN)—as core components of large-scale brain organization [1,2]. Since their introduction, however, each network has been defined and labelled in multiple, sometimes inconsistent, ways. For example, the DMN was originally described as "task-negative" in contrast to a "task-positive" system [3], but this designation has proven misleading, as DMN regions are active during diverse internally oriented and task-related processes [4]. Similarly, the SN has been variously referred to as the midcingulo-insular network, cingulo-opercular network, or ventral attention network, reflecting both anatomical parcellation schemes and theoretical emphases [5]. The CEN topologically overlaps substantially with what is elsewhere called the task-positive network (TPN) or the frontoparietal network (FPN), further blurring distinctions between control and attention systems [6]. The CEN and FPN have been considered to be subnetworks of the TPN [2], although discussions of the 3NM often use the CEN nomenclature when describing the tripartite framework.

These overlapping definitions reflect deeper methodological challenges. The 3NM itself has arisen in part due to magnetic resonance imaging (MRI) being the neuroimaging technique through which it was popularized [1]. Network assignment often depends on the atlas employed, the imaging modality, or the theoretical framework guiding interpretation [7,8,9,10,11]. For instance, cognitive neuroscience studies may emphasize functional distinctions (e.g., control vs. salience), whereas clinical work may adopt symptom-oriented labels [2,5]. Such variability complicates efforts to reconcile findings across modalities and disciplines. The goal of the present scoping review is therefore to synthesize recent evidence on the dynamics of the DMN, SN, and CEN, with attention to how methodological and taxonomic differences influence network definitions. We emphasize findings from functional magnetic resonance imaging (fMRI), electroencephalogram (EEG), magnetoencephalography (MEG) and positron emission tomography

(PET) with a particular focus on the role of temporal dynamics in shaping inter-network interactions [12,13,14].

The paper is organized as follows. We first review the 3NM and conduct an automatic analysis on the existing literature surrounding the 3NM. We then discuss the anatomical and functional connectivity (FC) labelling of brain regions followed by a discussion of the experimental and computational works reviewed, some of which derive effective connectivity (EC) measures. We then discuss neuroimaging modalities and their relevance to connectivity analysis. To summarize the literature survey, we synthesize traces of evidence in the literature that (i) SN's role is better characterized as context-dependent modulation; (ii) DMN engagement is task- and state-dependent rather than task-negative; (iii) what is often referred to as the CEN or FPN is a heterogeneous coalition or coordinated subnetworks. A table of nomenclature used can be found in Appendix Table 1. Our contribution is twofold: (i) a curated synthesis of results summarized in Appendix Table 2 (Ref. [6,12,14,15,16,17,18,19,20,21,22,23,24,25,26,27,28,29,30,31,32,33,34,35,36,37,38,39,40,41,42,43,44,45,46,47,48,49,50,51,52,53,54,55,56,57,58,59,60,61,62,63,64,65,66,67,68,69,70,71]), providing a structured map of disordered cognition, and (ii) a unifying interpretation of reported 3NM dynamics as manifestations of perturbed neural control. We conclude by positing that future taxonomies must integrate temporal dynamics and atlas differences to account for mechanisms across both time and spatial scales, respectively, and that this may be done by adopting the geometric control framework. A demonstrative example of this approach using a reviewed dataset is presented in Appendix Figs. 11,12 (Ref. [68]).

2. Literature Review

2.1 Semantic Analysis

Papers were selected from the results of a combination of PubMed (https://pubmed.ncbi.nlm.nih.gov/) (n = 41) and Scopus (https://www.scopus.com/) (n = 81) queries yielding 81 papers after deduplication (as of January 2026). The query searched across four neuroimaging modalities and for terms related to the 3NM:

((“Electroencephalography”[Mesh]) OR (“Magnetic Resonance Imaging”[Mesh]) OR (“Positron-Emission Tomography”[Mesh]) OR (“Magnetoencephalography”[Mesh]))

AND

((“functional connectivity” AND “triple network model” AND (“default mode network” OR “salience network” OR “central executive network”)))

Inclusion criteria included: (i) any articles whose titles or abstracts explicitly included any of the modalities (MRI = 41, EEG = 6, MEG = 2, PET = 3); (ii) any articles whose titles or abstracts explicitly included frequency bandwidth related terms (gamma = 0, beta = 3, alpha = 6, theta, delta = 4). A total of 55 papers were found to explicitly include these terms in abstracts, of which 9 were reviews. Fig. 1 shows a Preferred Reporting Items for Systematic reviews and Meta-Analyses (PRISMA)style [72] flowchart and a sunburst distribution of papers based on a regular expression search of terms.

A latent semantic analysis (LSA) [73] of the 81 abstracts was computed, producing a vector space representing the statistics of the word co-occurrences within the abstract corpora. A term frequency and inverse document frequency representation was used to weight terms and three different clustering algorithms were applied: (i) k-means, (ii) spectral clustering, and (iii) hierarchical density-based spatial clustering of applications with noise (HDBSCAN). This produced three separate groupings of the papers based on their latent semantics according to Euclidean centroid mass, graph-based and hierarchical-based clustering. Both k-means and spectral clustering require specifying the number of clusters (as centroids or top eigenvectors to project to). HDBSCAN requires specifying minimum cluster size in order to determine the number of clusters automatically, and outputs a noise/outlier category. A latent Dirichlet allocation (LDA) [74] was also computed, producing topic-word and document-topic distributions. The number of topics to model was chosen based on the results of a sweep over parameters (the number of topics and passes). Papers not labelled as outliers by the HDBSCAN were added to the selection yielding 64 papers. Appendix Figs. 8,9,10 show a comparison of clustering techniques used. Clustering generally reproduced obvious thematic groupings from the literature, with papers classified as HDBSCAN noise representing more transitional papers between these groupings (i.e., papers addressing multiple different kinds of disorders were found to be positioned between thematic clusters).

Topic modelling reveals related clusters of work: between resting state and task, across disorders, and with varying focuses on constituent parts of the 3NM. Some clusters are specific to disorders, with disorder clusters near to each other (likely due to the common language and possibly common network dynamics being reported). The 3NM has been applied to cognitive impairment ([15,16,17,18,19]), borderline personality disorder (BPD) [20,21], schizophrenia [22,23,24,25,26], affective disorders (AD) such as depression [27,28,29,30], obsessive-compulsive disorder (OCD) [31,32,33,34,39,75], substance use disorder (SUD) [35,36,37,38], attention-deficit/hyperactivity disorder (ADHD) [40], autism spectrum disorder (ASD) [41,42,43,44], post-traumatic stress disorder (PTSD) [45,46,47], Alzheimer's disease (AZD) and Parkin-

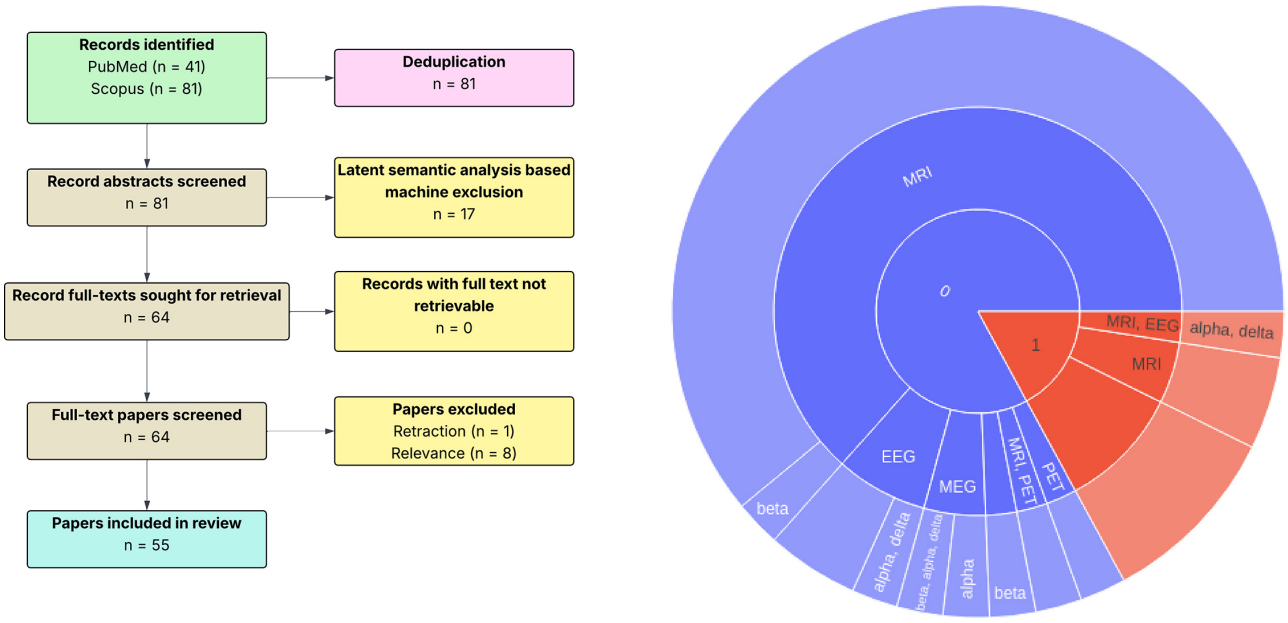

Fig. 1. Review flowchart. (Left) PRISMA-style identification, screening and inclusion based on automatic latent semantic analysis of abstracts and full text assessments. Right: distribution of explicit mentions between modality and bandwidth. (Right) A sunburst diagram showing the distribution of papers based on a naive text search using keywords. Blue (0) indicates a paper is a study, red (1) indicates a review (includes the keyword 'review' or 'survey' in abstract) and unlabelled arcs indicate no explicit references to terms of interest. PRISMA, Preferred Reporting Items for Systematic reviews and Meta-Analyses; MRI, magnetic resonance imaging; EEG, electroencephalogram; MEG, magnetoencephalography; PET, positron emission tomography.

son's disease (PKD) [48,49,50,51,52,53,54,55,56], pain [57,58,59,60], traumatic brain injury (TBI) [61,62,63], disorders of consciousness (DOC) [64], and problematic internet use (PIU) [65,66].

A manual citation based search yielded a further 7 studies with anatomical regions mapped to functional networks from the 3NM and sensorimotor networks. These networks are visualized in Fig. 2. A summary of results reviewed may be found in Appendix Table 2.

2.2 Modalities and Connectivity

The papers reviewed integrated different modalities of imaging as well as different brain atlases. Some were meta-analyses and/or reviews which considered more than one modality. Of the experiments reviewed, the most common modality was fMRI; MEG and PET studies were less common than EEG. The combined comparisons across modalities demonstrates the spatiotemporal resolution tradeoff involved when selecting a particular neuroimaging technique. This may be seen in the log-spatial vs log-temporal scales of different neuroimaging techniques in Fig. 3. In terms of temporal resolution, MEG/EEG is fastest (milliseconds) compared to fMRI (seconds) with better spatial resolution, and PET captures a similar spatial scale with a slower timescale [76]. For these reasons it is often helpful to integrate different modalities, accounting for multiple biological processes at play [77]. It is suggested that the reproducibility of associations within the brain requires a sample size on the order of hundreds [78] or thousands [79], however in the absence of such large cohorts, longer scan times and extensive repeated measures from the same subject help to improve prediction for smaller samples [80].

Functional MRI measures time-varying changes in blood flow during neural activity, captured through the blood-oxygen-level–dependent (BOLD) signal [81]. BOLD is a contrast mechanism used in fMRI. It reflects changes in blood oxygenation level that occur when neural activity increases/decreases in a brain region. The major strength of fMRI lies in its high spatial resolution, allowing fine-grained localization of brain activity and precise mapping of large-scale networks. However, this spatial precision comes at the cost of poor temporal resolution, as the hemodynamic response lags behind neuronal firing by several seconds representing several orders of magnitude difference in timescale with synaptic chemistry.

PET scanning uses a radioactive tracer to show typical and atypical metabolic activity [82]. The use of PET imaging exposes the patient to ionizing radiation and thus ethical and safety considerations limit repeated or longitudinal use, especially in vulnerable populations such as children or pregnant individuals. The development of these specific chemical tracers to target biochemical reactions of interest are also a constraint [83]. PET requires the synthesis of specific chemical tracers that target particular biochemical pathways or receptor systems—such as fluorine-18-fluorodeoxyglucose (i.e., 18F-FDG) for glu-

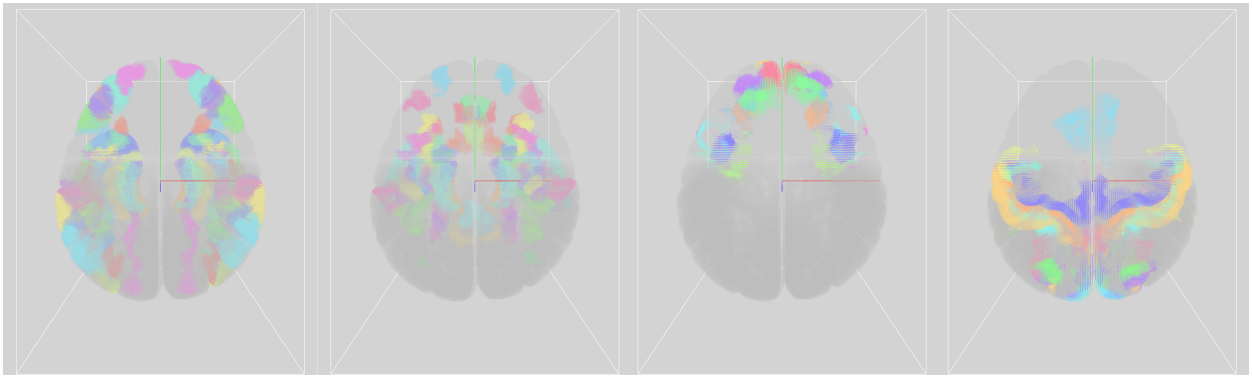

Fig. 2. Visualization of different reported functional networks. (From left to right) Default mode network, central executive/frontoparietal network, salience network, visual/sensorimotor networks. The highlighted regions are regions of interest that were identified in papers as interacting with the mentioned networks. We show all regions across all papers at once to show the distribution of regions and their annotations to functional networks.

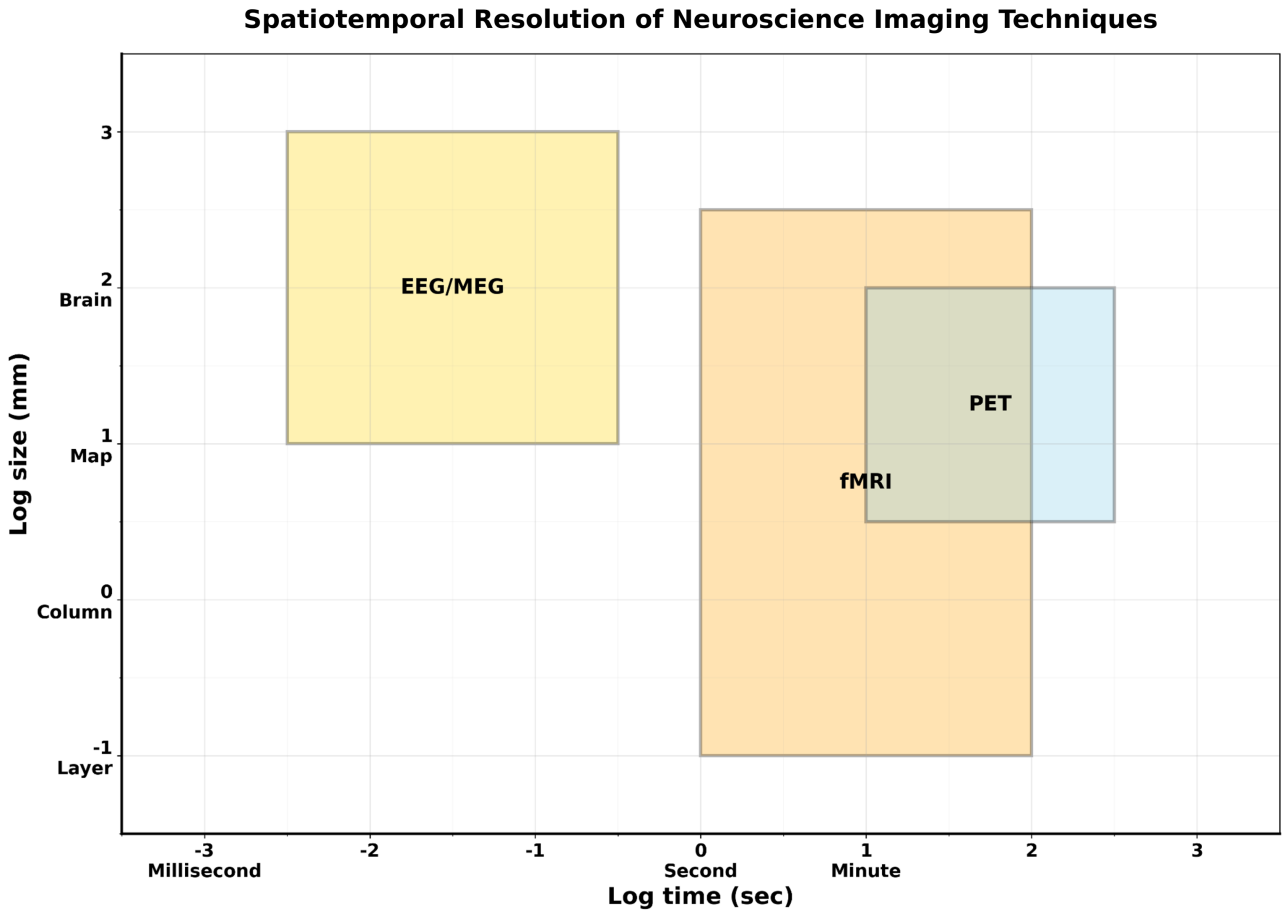

Fig. 3. Spatiotemporal relationship between modalities. The log-spatial and log-temporal resolutions of EEG, MEG, fMRI and PET. This demonstrates the tradeoffs when using different imaging modalities. Thus, a combination of modalities allows for larger coverage of this spatiotemporal space. fMRI, functional magnetic resonance imaging.

cose metabolism or carbon-11-raclopride (i.e., 11C-RAC) for dopamine receptor binding. The short half-lives of many isotopes necessitate onsite or nearby cyclotron facilities and rapid radiochemical synthesis, making PET both costly and logistically demanding. Despite these constraints, PET remains a powerful tool for investigating molecular and metabolic processes.

EEG records the brain's electrical activity through an array of electrodes placed on the scalp, capturing voltage fluctuations generated primarily by postsynaptic potentials

in cortical pyramidal neurons [13]. The method's non-invasiveness, relative affordability, and high temporal resolution make it a popular tool in both clinical diagnostics and cognitive neuroscience research. However, such surface measurements suffer from inherently poor spatial resolution because the recorded signals are distorted by volume conduction through the scalp, skull, and cerebrospinal fluid. The relationship between the underlying neural sources and the measured potentials, known as the EEG forward model, is complex and spatially diffuse. Consequently, estimating the distribution of cortical activity from scalp data, known as the inverse problem, is ill-posed and does not have a unique solution. To address this limitation, various computational approaches have been developed to improve source reconstruction accuracy, including minimum-norm estimation, beamforming, and Bayesian inference methods [84]. These techniques combine biophysical modelling of head conductivity with statistical regularization or prior information to estimate the most plausible distribution of brain activity consistent with the observed data.

MEG offers similar spatial and temporal resolution, however it measures magnetic activity rather than electrical. Using MEG, it has been shown that individual alpha frequency transcranial alternating current stimulation reduces static functional connectivity (sFC) across the DMN [54]. When FC derived from MEG is combined with clinical features, it has been shown to help identify atypical cases of self-limited epilepsy with centrotemporal spikes [85] (a focal epilepsy more common amongst children, otherwise known as benign Rolandic epilepsy [86]).

MEG and EEG both offer insights into the oscillatory activity of the brain that neither PET nor fMRI are able to physically capture but at the expense of spatial precision [87]. The reviewed studies demonstrate how these methods are applied in complementary ways to map brain function across a hierarchy of biological processes. The use of independent component analysis (ICA), a computational method separating mixed signals into statistically independent components, is a common tool within functional network identification. Although useful for preliminary analysis, it is often necessary to validate with more sophisticated techniques such as Bayesian or graph-based methods. When interpreting networks extracted using ICA, it is therefore important to consider both the imaging modality and brain atlas parcellation used in order to account for the spatiotemporal resolution at play. For this reason, multimodal approaches that integrate EEG and fMRI data have gained traction, as they can leverage the strengths of each modality. Recent reviews and perspectives show promise using multimodal and data fusion approaches [88,89,90]. Previously, simultaneous EEG and fMRI was used to link fluctuations in frontal theta power to BOLD activity in DMN hubs [12]. They found that found that frontal midline theta during a working-memory paradigm was negatively correlated with BOLD activity across multiple DMN regions such as the medial prefrontal cortex (mPFC), posterior cingulate cortex (PCC), inferior frontal–parietal cortices, middle temporal gyrus (MTG) and cerebellum. The authors posited either (i) a non-DMN theta generator, (ii) a medial-frontal source with network-wide coupling, or (iii) theta distributed throughout the DMN. The combination of EEG-fMRI [91] allows for a balanced trade-off between temporal and spatial resolutions [92,93].

Across modalities, a modulatory dimension emerges from oscillatory coupling. In EEG and MEG studies, FC is commonly estimated in the frequency domain using coherence [94] or phase analysis [95]. These metrics allow network coupling to be examined within specific oscillatory bands, revealing frequency-dependent subnetworks that do not necessarily align with BOLD-defined systems. Network coupling can be broadly categorized into either amplitude-amplitude coupling (AAC) or phase-amplitude coupling (PAC). AAC is the co-variation between two signals in terms of amplitudes, often describing functional connectivity where regions maintain synchronized activity rates. This kind of coupling suggests regions that are driven by a latent dynamic elsewhere, or are excitatorily connected to each other. PAC describes the covariation between the phase of a signal and the amplitude of another, where the timing of activity in one region synchronizes with the activity rate of another. This has been suggested to be the mechanism by which the SN switches, however validation by the alignment of different networks derived from different modalities remains an open problem. Early evidence reported BOLD correlates of EEG alpha phase-locking within the DMN [96]. Recent work has shown both AAC and PAC in EEG-fMRI signal coupling [97]. EEG has also been used to reconstruct dynamic, frequency-specific cortical networks using source analysis and ICA [67]. They identified five canonical networks with clear cross-frequency interactions: (i) an occipital visual network dominated by occipital alpha; (ii) a dual-process visual network showing anti-correlated alpha in the dorsal pathway and alpha/beta in the ventral pathway; (iii) a self-referential (anterior DMN) network with beta in the mPFC inversely coupled to alpha in the right temporoparietal junction (rTPJ); (iv) a memory–perception network characterized by precuneus alpha anti-correlated with ventral visual alpha; and (v) a sensori-motor network displaying beta–gamma coupling between post-central and pre-supplementary motor areas (pre-SMA) regions. Couplings such as the alpha-beta PAC between visual occipitotemporal cortex and ventral prefrontal cortex reflect an interaction whereby perceptual processes in alpha modulate higher-order recognition processes in beta. Similarly, beta-gamma PAC between the medial postcentral gyrus and pre-supplementary motor area supports the idea that lower-frequency sensorimotor rhythms modulate higher-frequency motor planning activity.

Source reconstruction [98] pipelines, comprising a forward head model in combination with an inverse solver,

play a critical role in shaping the apparent spatial organization of EEG/MEG-derived brain networks [99,100]. In these approaches, the forward model [101] characterizes how neural current sources within a realistic head volume give rise to sensor-level fields, typically using boundary element, finite element, or related numerical schemes constrained by individual or template MR images and tissue conductivity estimates. The inverse solver [84] then uses this biophysical mapping, together with prior assumptions and regularization constraints, to estimate a distributed pattern of source activity from a relatively sparse and noisy set of surface recordings. This two-stage procedure means that the spatial structure of any inferred network is not a direct reflection of the underlying neuronal generators, but instead emerges from the interaction between measurement geometry, forward modeling choices, and the statistical form of the inverse solution [102,103]. Assumptions about source orientation, depth weighting, and spatial smoothness, as well as the choice between minimum-norm [104], beamforming [105], Bayesian [106,107], or sparsity-promoting estimators [108], can systematically influence the apparent extent, localization, and covariance structure of reconstructed sources [109]. For example, minimum-norm methods such as low-resolution electromagnetic tomography (LORETA) [110] assume distributed activities and produce smooth activity topographies whereas beamforming methods assume activities with localized and focal specificity. As a result, features such as the degree of spatial dispersion of hubs, the apparent long-range connectivity between regions, or the segregation of networks into distinct spatial modules can all be shaped by the specific forward–inverse pair employed rather than solely by neuronal physiology. In practice, therefore, source reconstruction pipelines should be regarded as spatial filters that transform scalp-level signals into volumetric images of brain activity, and careful evaluation, comparison, and validation of different pipelines are essential when drawing conclusions about the large-scale organization of functional networks. This is particularly important when considering the interactions between purported networks such as SN switching, where attribution of large-scale networks should be validated against multiple different source reconstructions and atlas parcellations.

The characterization of large-scale brain networks within the 3NM depends critically on the modality and computational methods used to estimate connectivity, extract network structure, and quantify inter-network interactions. Across the literature reviewed, functional and effective connectivity were derived using a diverse set of statistical, graph-theoretic, and dynamical systems approaches, each imposing distinct assumptions about neural coupling, temporal stationarity, and causality. These methodological choices substantially influence the resulting network topology, connectivity and inferred roles of the DMN, SN and CEN. The most common operationalization of FC in fMRI studies is Pearson correlation between regional BOLD time series, using the sFC matrix to represent average co-fluctuations over a minutes-long timescale. Variants include using partial correlation to control for indirect effects [111], and regularized covariance estimation [112] to mitigate noise in high-dimensional parcellations. These approaches implicitly assume stationarity and linear dependence, yielding a time-averaged view of network structure that favors stable spatial patterns.

To capture temporal variability, many recent studies employ dynamic functional connectivity (dFC), typically using sliding-window correlations, tapered windows, or time–frequency coherence [113,114]. Recent reviews and perspectives on this approach emphasized the challenge of interpretability being a common theme [115,116,117]. These methods reveal transient connectivity states in which DMN–CEN antagonism or SN-driven switching is more pronounced. However, dFC is not without its limitations. Window length selection strongly constrains the temporal resolution of the analysis, which characterizes the timescale in which brain states can be detected. Different parameterizations of the dynamic windowing thus yield divergent network states, contributing to inconsistencies across reports. Therefore, the parameter spaces and sweeps done during the network state identification process should always be noted and taken into consideration with downstream results.

Functional connectivity, static or dynamic, statistically describes the co-occurrence of activity agnostic to modality. This is contrasted against effective connectivity which addresses directionality [118]. Where sFC and dFC differ in their treatment of the temporal dimension, EC and FC differ in the treatment of causal influence. For a current window in time, dFC models the statistics across multiple region based channels. FC reflects statistical co-fluctuations between brain regions without implying direction, simply that regions are active together in some pattern, whereas EC aims to capture directed causal influence and the mechanisms by which one region drives another [118]. Intrinsic FC or EC often refers to coordinated network activity across different cognitive states, usually derived from resting state data. EC approaches such as Granger causality (GC) [119] detect directed influences by testing if past values of one region's signal predict another's beyond its own autoregression, naturally handling lags across sliding windows. In addition, hidden state biophysical models may be included for investigating biologically plausible mechanisms [68]. Such approaches extend beyond static correlations by incorporating temporal dynamics, often using generative processes to estimate causal pathways while accounting for network effects. Dynamic causal modelling (DCM) [120] uses Bayesian inversion of biophysical state-space models to estimate directed coupling between hidden neuronal states, explicitly modeling hemodynamics and inputs. GC and DCM has been found to infer similar directionality between the posterior cingulate cortex, the

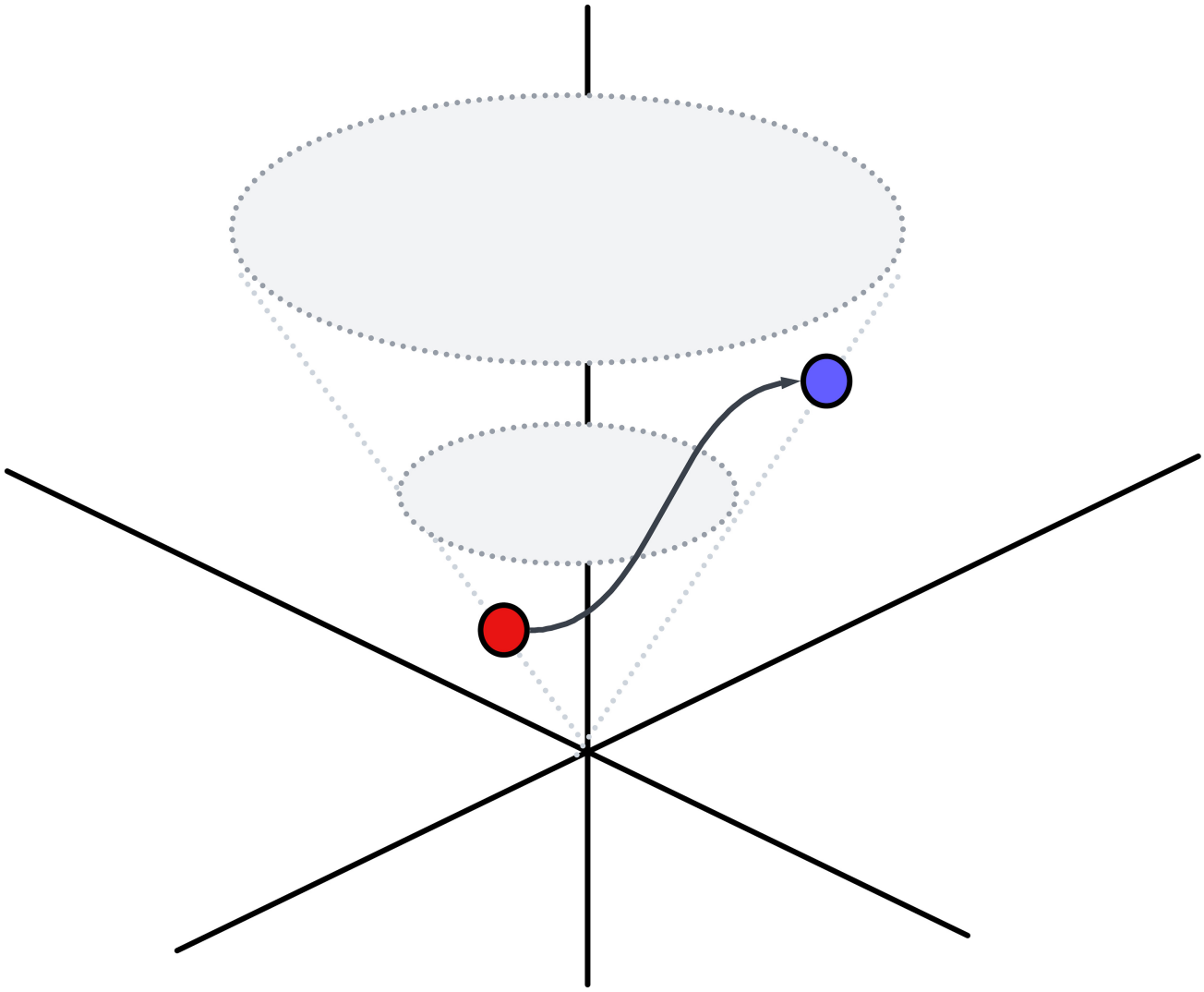

Fig. 4. Simple diagram of SPD geodesics. In low dimensions, SPD matrices live inside a cone, and geodesics are optimal paths between points that minimize energy given the metric chosen. Paths using Euclidean geometry cut outside of the space and thus produce a trajectory that does not remain in the cone, and thus outside the range of valid brain signal covariance configurations. SPD, symmetric positive-definite.

medial prefrontal cortex, the left middle temporal cortex, and the left angular gyrus [121]. High temporal resolution modalities such as EEG are particularly well suited to estimating effective connectivity because they can resolve rapid, transient interactions underlying cognitive control. High-density EEG with source reconstruction and further refinement using recursive sparse Bayesian learning has also been used to estimate effective connectivity among SN nodes during attention switching [14]. Participants solved multiple-choice problems that required shifting between internally and externally oriented cognition. The analysis showed that EEG-based source modeling can recover directed SN interactions, with rAI acting as a salience hub and right anterior insula–anterior cingulate cortex (rAI–ACC) coupling supporting state switching. Externally oriented episodes engaged the CEN and suppressed the DMN, consistent with canonical task versus rest dynamics.

2.3 Anatomical Labellings and Brain Atlases

Whether mapping out functional networks (clusters of regions coordinating together) or effective influence (which networks affect and are affected by other networks), some parcellation of the brain volume is required. To these ends, computational methods are grounded in standardized brain atlases [122] which enable comparisons between studies [123]. Most existing network labelling and taxonomic frameworks have been developed around spatial and functional criteria [124,125], including connectivity, architectonics, and topographic organization [126] and is often an automated process [127]. Modern multiscale brain modelling [128] seeks to parcellate and group anatomical regions across multiple spatial and biologically structured scales. A systematic review of whole brain MRI atlases [129] includes caveats for population imaging. More re-

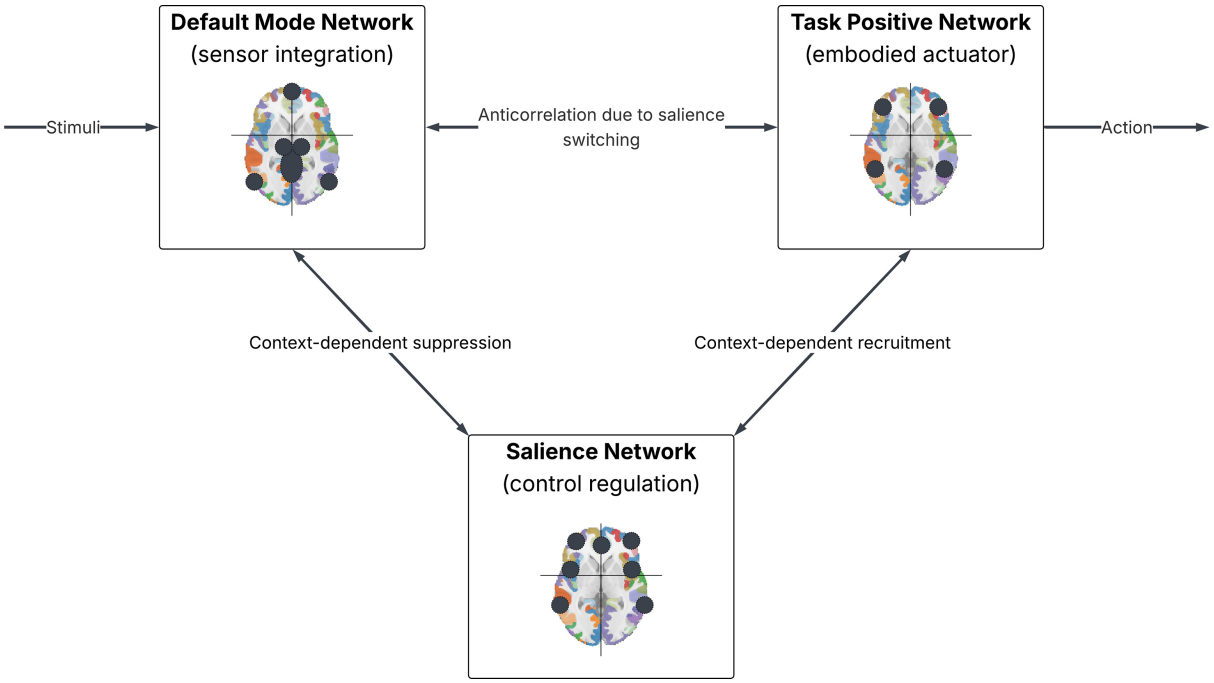

Fig. 5. The 3NM interpreted as a control loop. 3NM interpretation as a control system closing an embodied loop. Here, the DMN acts as a sensor integrator reconciling different sources of perceptual stimuli with the current state, the SN acts as a controller dynamically suppressing and recruiting different regions, and the TPN acts as an actuator engaging with motor systems. 3NM, triple network model; DMN, Default Mode Network; SN, Salience Network; TPN, task-positive network.

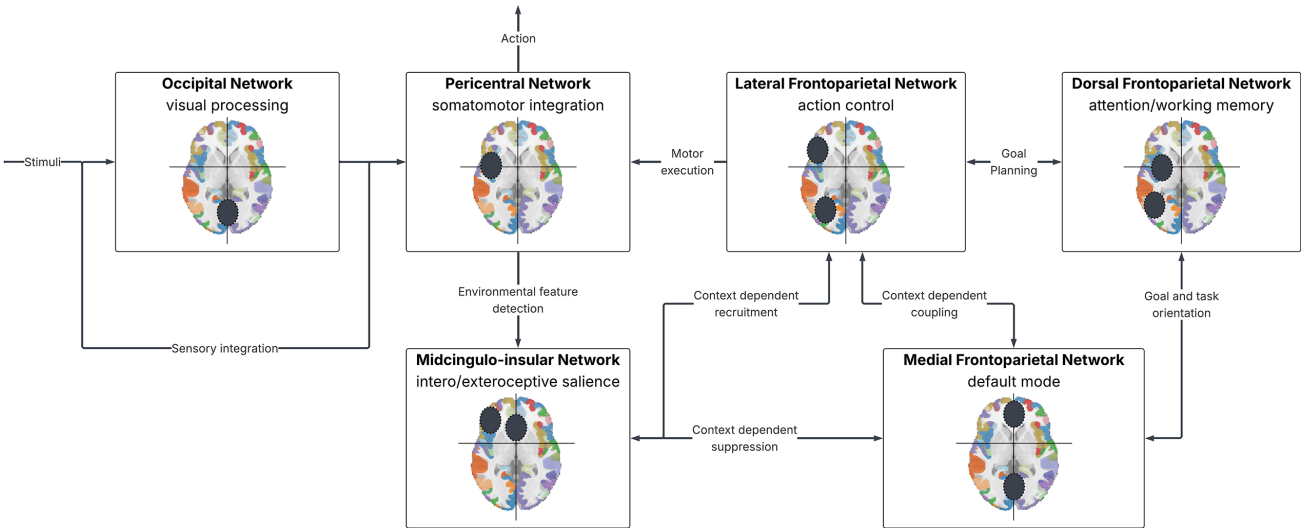

Fig. 6. The macro-scale network parcellation [5] interpreted as a control loop. A larger parcellation of functional networks allows for a more descriptive control system. Here, a similar embodied loop is closed, however different regions have more detailed interactions than the 3NM interpretation.

cent surveys have comprehensively catalogued and standardized available brain atlases [130] and chronicled their historical development [131]. By contrast, the temporal dimension of neural mass activity (manifest in oscillatory dynamics, cross-frequency coupling, and transient synchronization across modalities) has received relatively less focus. Placing greater emphasis on temporal properties as an organizing dimension permits researchers to conceptualize neural networks not only in terms of spatial and functional specificity but also as dynamic systems whose rhythmic and state-dependent patterns contribute centrally to cognition [132].

The structure of atlases depends on the data used and research goals, e.g. across age or specific diseases such as schizophrenia [133]. In this review, we focus primarily on the Montreal Neurological Institute (MNI) stereo-

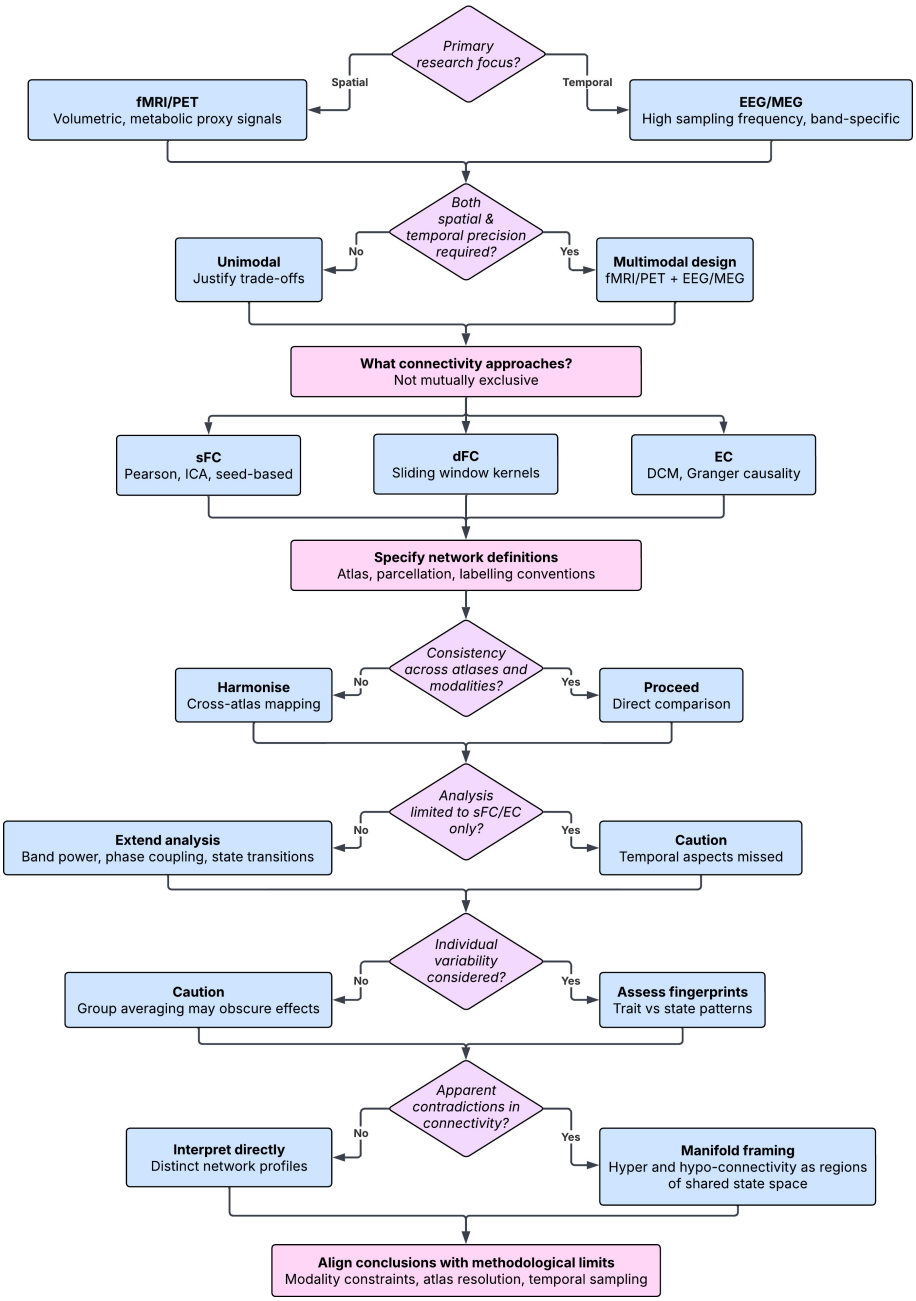

Fig. 7. A proposed workflow for connectivity analysis. The workflow incorporates the selection of different modalities, the trade-off between spatial and temporal resolution, the parcellation of brain atlases with network definitions, as well as constraints for analysis such as individual precision and contradicting connectivity. sFC, static functional connectivity; ICA, independent component analysis; dFC, dynamic functional connectivity; EC, effective connectivity; DCM, dynamic causal modelling.

taxic space and the Human Connectome Project multimodal parcellation (HCP-MMP) atlas. The HCP-MMP is a multimodal cortical parcellation dividing the cerebral cortex into 360 areas (180 per hemisphere) based on structural, functional, and connectivity features [7]. The extended Human Connectome Project multimodal parcellation (HCPex) extension is an expansion of HCP-MMP that includes subcortical thalamic structures, enabling whole-brain analyses beyond the cortex [9]. With such atlases, modality integration benefits from including volumetric measurements that are able to capture subcortical activity. Additional atlases and tools employed in the studies reviewed include Desikan–Killiany (DK) cortical parcellation, the Yeo-7 atlas [134] and various MNI-based atlases. The DK atlas [8] is a gyral-based cortical parcellation comprising 68 regions, succeeded by the Desikan-Killiany-Tourville (DKT) atlas [135], which refines the DK parcellation to improve anatomical accuracy and compatibility with neonatal brain templates. The Yale Brain Atlas [136] provides a high-resolution cortical parcellation with subgyral localization.

Table 1. Abbreviations and initialisms.

Abbreviation	Full name	Notes
PRISMA	Preferred Reporting Items for Systematic reviews and Meta-Analyses	Guidelines for conducting systematic reviews
(f)MRI	(Functional) Magnetic Resonance Imaging	Imaging modality
rs-fMRI	Resting State fMRI	
BOLD	Blood-Oxygen-Level-Dependent	Proxy for metabolic activity
DTI	Diffusion Tensor Imaging	Imaging modality
(i)EEG	(Intracranial) Electroencephalogram	Imaging modality
MEG	Magnetoencephalography	Imaging modality
PET	Positron Emission Tomography	Imaging modality
18F-FDG	Fluorine-18-Fluorodeoxyglucose	PET agent
11C-RAC	Carbon-11-Raclopride	PET agent
WM	Working Memory	
EM	Episodic Memory	
(s/d/i)FC	(Static/Dynamic/Intrinsic) Functional Connectivity	Synchronous activity between regions of interest
EC	Effective Connectivity	Directed influence activity between regions of interest
GC	Granger Causality	Method for measuring predictability of a series given a different series
DCM	Dynamic Causal Modelling	Method for estimating directed influence between regions of interest
AAC	Amplitude-Amplitude Coupling	Covariation between two signal envelopes and their amplitude
PAC	Phase-Amplitude Coupling	Covariation between phase of a signal with the amplitude of another
MNI	Montreal Neurological Institute	Standardized template for reporting coordinates in neuroimaging studies.
DK	Desikan-Killiany	68 gyral-based cortical regions. Alternative names may appear across studies. Proposed networks assigned post hoc based on functional mapping.
HCP-MMP	Human Connectome Project Multimodal Parcellation	360 cortical areas (180 per hemisphere) based on structure, function, and connectivity.
HCPex	Extended Human Connectome Project Multimodal Parcellation	HCP-MMP extended with 66 subcortical regions
LSA	Latent Semantic Analysis	Method to analyze word co-occurrences based on distributional semantic hypothesis
LDA	Latent Dirichlet Allocation	Method to analyze latent topics based on distributional semantic hypothesis
HDBSCAN	Hierarchical Density-Based Spatial Clustering of Applications with Noise	Method to cluster points that returns an outlier class
UMAP	Uniform Manifold Approximation and Projection	Method for stochastically reducing dimensions
ICA	Independent Component Analysis	Method separating mixed signals into statistically independent components
PCA	Principal Component Analysis	Method for separating mixed signals into components explaining variability
PTE	Phase-Transfer Entropy	Method for measuring directed connectivity
RSBL	Recursive Sparse Bayesian Learning	Method combining recursive updating and Bayesian sparsity constraints applied to source reconstruction
DTF	Directed Transfer Function	Method for measuring directed connectivity
SPD	Symmetric Positive-Definite	Space of symmetric matrices with positive eigenvalues
AIM	Affine-Invariant Metric	
LEM	Log-Euclidean Metric	
LCM	Log-Cholesky Metric	

Table 1. Continued.

Abbreviation	Full name	Notes
BWM	Bures-Wassserstein Metric	
PGA	Principal Geodesic Analysis	Generalization of PCA using geodesics
BCI	Brain-Computer Interface	
BPD	Borderline Personality Disorder	
AD	Affective Disorder	
MDD	Major Depressive Disorder	
OCD	Obsessive-Compulsive Disorder	
SUD	Substance Use Disorder	
AUD	Alcohol Use Disorder	
CUD	Cocaine Use Disorder	
TUD	Tobacco Use Disorder	
ADHD	Attention-Deficit/Hyperactivity Disorder	
ASD	Autism Spectrum Disorder	
PTSD	Post-Traumatic Stress Disorder	
AZD	Alzheimer's Disease	
TBI	Traumatic Brain Injuries	
DOC	Disorders of Consciousness	
PIU	Problematic Internet Use	
3NM	Triple Network Model	
DMN	Default Mode Network	
SN	Salience Network	
TPN	Task-Positive Network	
CEN	Central Executive Network	
FPN	Frontoparietal Network	
ECN	Executive Control Network	
DAN	Dorsal Attention Network	
ACN	Anterior Control Network	
VAN	Ventral Attention Network	
VFN	Ventral Frontoparietal Network	
VAS	Ventral Attention System	
ON	Occipital Network	HCP-MMP cortical regions
PN	Pericentral Network	
D-FPN	Dorsal Frontoparietal Network	
L-FPN	Lateral Frontoparietal Network	
M-FPN	Medial Frontoparietal Network	
M-CIN	Midcingulo-Insular Network	
Primary_Visual	Primary visual	
Early_Visual	Early visual	
Dorsal_Stream_Visual	Dorsal stream visual areas	
Ventral_Stream_Visual	Ventral stream visual areas	
MT+_Complex	Middle temporal and medial superior temporal complex and neighboring visual areas	
SomaSens_Motor	Somatosensory and motor	
ParaCentral_MidCing	Paracentral mid cingulate	
Premotor	Premotor	
Posterior_Opercular	Posterior opercular	
Early_Auditory	Early auditory	
Auditory_Association	Auditory association	
Insula_FrontalOperc	Insula and frontal opercular	
Medial_Temporal	Medial temporal	
Lateral_Temporal	Lateral temporal	

Table 1. Continued.

Abbreviation	Full name	Notes
TPO	Temporo-parieto-occipital junction	
Superior_Parietal	Superior parietal lobule	
Inferior_Parietal	Inferior parietal lobule	
Posterior_Cingulate	Posterior cingulate cortex and splenial	
AntCing_MedPFC (ACC)	Anterior cingulate and medial prefrontal cortex	
OrbPolaFrontal	Orbitofrontal and polar frontal	
Inferior_Frontal	Inferior frontal	
Dorsolateral_Prefrontal	Dorsolateral prefrontal	
BA	Brodmann Area	
rAI-ACC	Right Anterior Insula - Anterior Cingulate Cortex	
dACC	Dorsal-Anterior Cingulate Cortex	
mPFC	Medial Prefrontal Cortex	
PCC	Posterior Cingulate Cortex	
MTG	Middle Temporal Gyrus	
rTPJ	Right Temporoparietal Junction	
(pre)-SMA	(Pre-) Supplementary Motor Area	

The Yeo-7 coarse parcellation estimates 7 cortical networks based on MRI data from 1000 subjects. The MNI is a standardized coordinate system derived from averaged MRI templates, widely used to align and compare results across studies. The MNI 152 is a population-averaged template created from 152 T1-weighted MRI scans, serving as the most common reference brain in neuroimaging [10]. The MNI Colin 27 is a high-resolution single-subject template generated from averaging 27 T1-weighted MRI scans of the same individual, used for precise anatomical localization [11]. Recent work such as PaleoArchiNeo [137], a gyral-based atlas, parcellates the cortex into 5 broad regions composed of 30 subregions of interest using a phylogenetic approach, producing a progression of cortical regions based on evolutionary development. We may thus broadly evaluate atlases on their anatomical, functional and evolutionary considerations when templating volumes of the brain. Platforms such as NeuroVault [138] provide researchers with an open repository of brain parcellations to encourage scientific reproducibility. These atlases can be viewed in softwares such as FreeSurfer [139] or volBrain [140], although there have been reported inconsistencies in cortical thickness across these tools [141].

Importantly, we highlight the conceptual work of constructing taxonomies for functional connectivity [5]. A recent approach is the "macro-scale" naming convention to alleviate some of the confusion surrounding network labelling and function [5]. This report identifies one of the common problems the authors faced while trying to consolidate the information: different naming conventions and sometimes even different functions assigned to overlapping networks. For example, previously, task-positive or control network labels often combined frontoparietal and dorsal attention systems into a single category [142]. The macro-scale approach [5] outlines how functional networks are currently defined, suggesting a common taxonomy of six large-scale anatomical-functional networks. The proposed cortico-centric networks are: (i) occipital network (ON), (ii) pericentral network (PN), (iii) dorsal frontoparietal network (D-FPN), (iv) lateral frontoparietal network (L-FPN), (v) midcingulo-insular network (M-CIN), (vi) medial frontoparietal network (M-FPN). According to their anatomical-functional approach, at the current state of knowledge, the most appropriate ways to define functional networks are by either (a) resting state functional connectivity or (b) task-activation and meta-analysis. This, combined with a recent set of ten recommendations when conducting neuroimaging-based meta-analyses [143], provides a flexible approach to interpreting functional connectivity and the network taxonomies often reported.

2.4 Salience Network Modularity

The CEN and DMN display antagonistic dynamics: during externally oriented tasks, dorsolateral prefrontal and posterior parietal regions (i.e., CEN related regions) are engaged while medial prefrontal and posterior cingulate regions (i.e., DMN related regions) are suppressed [142]. This reciprocal relationship is modulated by SN signals, with rAI–ACC coupling acting as a gatekeeper for network switching [69]. An advantage of EEG over fMRI is its millisecond temporal resolution, though scalp recordings suffer from low spatial precision and noise. Intracranial EEG (iEEG) provides both higher spatial resolution and better signal-to-noise ratio at the expense of invasivity [144]. Using this modality, phase-transfer entropy (PTE) and high-gamma (80–160 Hz) measures have been used to probe directed interactions among regions within the SN, DMN, and FPN during both verbal and spatial memory processing [69]. Memory traces are thus generated by attentional enhancement which selects and then modulates which neural

patterns encode/recall episodic information. PTE revealed a consistent causal outflow from the anterior insula (SN) toward DMN and FPN nodes, identifying it as a key control hub. High-gamma analyses showed selective DMN suppression, with PCC/precuneus activity reduced during encoding but not recall, reflecting context-dependent engagement of the network.

DMN suppression during resting state may better be understood when considering mind wandering, where attention shifts inward to unrelated thoughts. A seminal meta-analysis of fMRI (and one PET) studies of mind-wandering showed that spontaneous thought consistently engages a distributed set of regions dominated by the DMN, with additional recruitment of prefrontal and insular areas [4]. The analysis demonstrated that DMN hubs provide the core substrate for spontaneous cognition, aligning with evidence that these regions support internally directed thought. Although the review does not commit to a formal parcellation, the pattern is consistent with medial-temporal and dorsal-medial DMN subdivisions linked to memory-based and social–self-referential processes, with mPFC and PCC acting as integrative hubs. The implication is that these regions combine and coordinate information in relation to the identified cognitive processes. Mind-wandering thus appears to rely on intrinsic DMN activity [145] combined with flexible coupling to FPN regions [146], supporting both spontaneous generation and top-down modulation of internal mentation. The presence of reliable activations outside the DMN–FPN axis—particularly in somatosensory cortex, insula, lingual gyrus, and temporopolar cortex—indicates that sensory, interoceptive, and imagery-related processes are routinely embedded within spontaneous thought [147], consistent with first-person reports of visual and bodily imagery during mind-wandering [148,149].

2.5 Default Mode Dynamism

Increasing converging evidence suggests that DMN is not a static representation of self-referential thought but a collection of dynamic processes exhibiting metastable substates which have also been shown to have competitive couplings with other networks in the beta band [42,150]. These metastable substates represent different activation profiles that emerge from global functional integration [151]. Network metastability is thought to arise as a dynamic balance between synchronization and independent activities across regions. A recent perspective review [152] presented a comprehensive conceptual overview, with the separate scoping review [153] highlighting existing empirical operationalizations. It has been shown that the FPN modulates alpha band activity in downstream visual association cortices, whereas the cingulo-opercular network showed no evidence for such top-down modulation, highlighting a selective role for FPN in biasing sensory processing [6]. Moreover, FPN activity maps preferentially onto slower-frequency oscillations (4–14 Hz), supporting its role as a flexible hub coordinating inter-network activity. By contrast, the DAN exhibited greater coupling between alpha band power and BOLD, whereas the FPN showed stronger coupling in the theta band (3–8 Hz), further suggesting functional dissociation across control subnetworks. In terms of DMN-specific modulation, frontal theta activity was found to be negatively correlated with BOLD in DMN hubs such as the medial prefrontal cortex and precuneus [12]. Three explanatory accounts have been proposed: (i) frontal theta reflects an external control system that suppresses DMN activity, (ii) the DMN contains a theta-generating hub, or (iii) theta represents an intrinsic modulatory rhythm of the DMN itself. Together, these possibilities highlight ongoing debates about the exact mechanism of DMN suppression.

2.6 Central Executive Heterogeneity

There exists activity heterogeneity within the FPN as well. The FPN functions as a flexible control hub whose electrophysiological signature is dominated by low-frequency theta/alpha rhythms (4–14 Hz) that support long-range coordination during both rest and task [6]. These slower oscillations show the strongest correspondence with FPN BOLD activity and help distinguish it from nearby attention networks, which rely more heavily on alpha-band dynamics. The findings also stress that the FPN's spatial layout is highly individualized, so its oscillatory–BOLD relationships can only be meaningfully interpreted using precision, subject-specific network mapping rather than group averages. This reinforces the suggestion that multimodal approaches are necessary, as fMRI provides the spatial resolution that EEG lacks. Evidence of subsystem differentiation has been found in regions associated with the CEN, and even at the individual level, sensitivities in executive network resting state FC. Specifically, there is heterogeneity in the frontoparietal control networks, each with different couplings to DMN and DAN regions [154], concurrent with existing parcellations [5]. This heterarchy of connectivities between different regions of the brain is a task-dependent dynamic organization [155] of network recruiting and coactivations. An image based meta-analysis revealed four distinct topological networks that were identified across the literature but inconsistently labelled: FPN, executive control network (ECN), dorsal attention network (DAN), and TPN [156]. We adopt their recommended secondary labels for each network: DAN, left and right CEN, and anterior control network (ACN). Together, these form the topologically distinct networks reported to engage in executive control. Both the DMN [157] and SN also exhibit context-dependent heterogeneity of dynamics. The DMN has also been found to exhibit heterogeneity during social, episodic and self-referential thought [158]. More recent work has found that the DMN is not a unitary functional network but it includes three subsystems at the group level and two distinct default networks at the individual level [159]. The SN has also been shown to be heterogeneous across the senso-

Table 2. Summary of studies reviewed.

Cognitive phenomenon/condition	Source, task paradigm, modality, cohort/review size	Computational approach and connectivity analysis	Reported network interactions
Non-disordered cognition	[12] Working memory task using EEG-fMRI 20 right-handed, healthy participants (17 females, 3 males)	Frontal theta EEG with ICA for BOLD-oscillatory correlation	Theta-linked modulation of somatosensory regions Frontal theta inversely tracks DMN BOLD signals
	[67] Resting state EEG-fMRI 80 healthy participants	Source localization with ICA for FC across frequency bandwidths	Precuneus alpha anti-correlated with ventral visual alpha Medial prefrontal cortex beta anti-correlated with temporoparietal junction alpha Dorsal visual alpha anti-correlated with ventral visual beta Medial postcentral gyrus beta correlates with pre-supplementary motor area gamma
	[69] Four diverse episodic memory tasks involving spatial and verbal encoding and recall compared to resting state iEEG 177 participants	Phase-Transfer Entropy in high gamma band for EC	DMN suppressed during encoding but not recall Anterior insula sends influence to FPN Anterior insula causally influences DMN and FPN
	[6] Various memory and cognitive task states compared to resting using EEG and fMRI	Narrative review of cross-correlated BOLD/EEG couplings	FPN uses low-range frequency for long range (coupled with BOLD in theta band), acts as flexible hub during different tasks
	[14] Attention switching between internal/external tasks using EEG 25 healthy participants (13 females, 12 males)	Recursive sparse Bayesian learning for EC	Dorsolateral prefrontal cortex and posterior parietal cortex engaged during external task while medial prefrontal cortex and posterior cingulate cortex suppressed Right anterior insula key hub for identifying salient events Right anterior insula and ACC effective coupling regulates switching
	[68] Working memory task encoding geometric and word stimuli using EEG 15 healthy participants (11 females, 4 males)	RNN based EC on HCP-MMP parcellation of LORETA source reconstruction	Connectivity patterns suggest SN has modulatory role between DMN and CEN
Cognitive impairment	[18] Neuropsychological tests compared to rs-fMRI 66 hemodialysis patients 66 healthy controls	ICA for triple network, sliding window and k-means for dFC	Anterior/posterior DMN, left/right CEN, SN
	[19] Cognitive test scores compared to rs-fMRI 41 post-stroke cognitive impairment 41 healthy controls	Spectral DCM for EC	Changes in EC from posterior cingulate cortex to dorsolateral prefrontal cortex negatively correlated with cognitive scores

Table 2. Continued.

Cognitive phenomenon/condition	Source, task paradigm, modality, cohort/review size	Computational approach and connectivity analysis	Reported network interactions
Borderline personality disorder (BPD)	[20] Clinically observed 'stable instability' of emotions from rs-fMRI 14 patients 16 healthy controls	High order ICA to extract spatiotemporal patterns of coherent BOLD signals and intra/inter-intrinsic FC	Aberrant intra-iFC between 3NM Inter-iFC of CEN decreased, inter-iFC of SN increased
	[21] rs-fMRI review 15 studies	Seed-based and ICA-derived dFC Sliding window and clustering	SN dysfunction impairs DMN-CEN switching, linking to attentional deficits Altered DMN-CEN coupling associates with rumination (DMN dominant for addiction)
Schizophrenia	[22] rs-fMRI 20 patients schizophrenia 20 patients depression 20 healthy controls	Seed-based FC analysis with GC	Patient groups showed same abnormal causal connectivity between DMN-SN Opposing aberrant FC of DMN-CEN (increased in schizophrenia) and SN-CEN (increased in depression)
	[23] rs-fMRI 37 patients first-episode psychosis (FEP) 78 patients clinical high risk psychosis (CHR-P) 110 healthy controls	ICA and mediation analysis for FC	FEP and CHR-P had lower SN-DMN and SN-CEN connectivity
	[24] Resting state review of EEG and fMRI 21 studies	FC	Abnormal SN-DMN and SN-FPN coupling Reduced DMN-FPN connectivity Increased intra-network connectivity within DMN and FPN Altered beta/gamma activity and impaired modulation of cortical synchrony linked to self-disorder severity
	[25] Synthesis review of EEG, MEG, fMRI, PET	iFC	Presents integrative model of 3NM and prediction errors in the SN, aberrant salience and dopamine for cognitive control system
	[26] Resting state EEG 30 patients chronic schizophrenia 30 healthy controls	Source localization based DTF for EC	Disturbances across frequency bandwidths within 3NM Multiband DMN hyperconnectivity, low-band hyper- and high-band hypoconnectivity in CEN, reversed direction of information flows in SN at theta/beta bands
	[70] Self-reported psychopathology data compared to rs-fMRI 922 youth and early adults	Network segregation metrics	Subgroups identified using SN segregation scores

Table 2. Continued.

Cognitive phenomenon/condition	Source, task paradigm, modality, cohort/review size	Computational approach and connectivity analysis	Reported network interactions
Affective/mood disorders (AD) such as major depression disorder (MDD) or bipolar disorder (BD)	[27] rs-fMRI 38 unmedicated BD 35 unmedicated MDD patients during depressive episodes 47 healthy controls	ICA and FC	Both the BD and MDD patients showed shared weaker intra-network FC in the left mPFC and right precuneus within the DMN as well as weaker inter-ROI FC between the left AI and right AI compared with the healthy controls BD had weaker while the MDD had stronger intra-network FC in the right dlPFC within the rCEN as well as stronger inter-region FC between the right dlPFC and right ANG compared with the healthy controls BD showed specific, stronger inter-ROI FC between the left PPC and right AI as well as stronger inter-network FC between the lCEN and SN compared with either the MDD or the control group.
	[28] rs-fMRI 51 unmedicated depressed BDII patients 51 unmedicated depressed MDD patients 52 healthy controls	ICA, sliding window correlation and k-means clustering for dFC	3NM dFC clustered into four configuration states, three of them showing dense connections and the other sparse connections Both BD and MDD patients spent more time in sparse state and showed decreased dFC variability between posterior DMN and rCEN compared with controls MDD patients showed specific decreased dFC variability between anterior DMN and rCEN compared with controls
	[29] rs-fMRI 158 young participants with major AD (101 with current suicidal ideation, 57 without) 64 age- and sex-matched healthy control individuals	Seed-based connectivity analysis adjusted by diagnoses and prior suicide attempts	CSI group exhibited hyperconnectivity between the anterior insula (SN) and hippocampus, between the posterior parietal cortex (FPN) and rectus gyrus (DMN), between the amygdala (SN) and cerebellum Both CSI and non-CSI groups exhibited increased FC between the posterior parietal cortex and emotional perception-related regions, specifically, the superior and middle temporal gyri, compared with healthy control individuals.
	[30] rs-fMRI 248 older adults with cognitive symptoms 95 older adults with depressive symptoms	Seed-based connectivity analysis	Identified regions across 3NM associated with cognitive decline and late-life depression
Obsessive-compulsive disorder (OCD)	[39] rs-fMRI 35 patients 32 healthy controls	ICA for FC	OCD patients demonstrated aberrant functional interactions between SN and anterior DMN; between SN and dorsal CEN Interaction between the SN and dorsal CEN significantly correlated with trait anxiety level in the OCD group

Table 2. Continued.

Cognitive phenomenon/condition	Source, task paradigm, modality, cohort/review size	Computational approach and connectivity analysis	Reported network interactions
	[31] Meta-analysis of seed-based rs-fMRI 18 studies (541 patients, 572 healthy controls)	Seed-based connectivity analysis for iFC	Altered connectivity within 3NM and between-network hypoconnectivity supports aberrant fronto-striatal model of OCD
	[32] rs-fMRI 49 patients 41 healthy controls	ICA and sliding window FC	Dysconnectivity between the left and right FPN, between the left FPN and SN
	[33] Systematic review of resting and task state EEG and fMRI 166 studies (10 EEG, 156 fMRI)	Quantitative analysis	OCD exhibited lower connectivity in delta and alpha EEG bands, with inconsistent findings in other frequency bands Resting state fMRI studies reported conflicting connectivity patterns within the DMN and sensorimotor cortico-striato-thalamo-cortical circuitry Decreased resting state connectivity between the DMN and SN Task-related hyperconnectivity within the DMN-SN and hypoconnectivity between the SN and FPN suggesting cognitive inflexibility
	[34] rs-fMRI 88 medication-free OCD patients 93 healthy controls	ICA combined with sliding window and k-means clustering for s/dFC Spectral DCM and parametric empirical Bayes framework for abnormal EC	Weakened sFC between the left and right FPN Time-varying hypoconnectivity patterns between left FPN and DMN, between right FPN and SN
Attention-deficit/hyperactivity disorder (ADHD)	[40] rs-fMRI 140 children with ADHD (80 primary cohort, 60 replication cohort)	ICA and SN-centered network interaction index for cross-network coupling measurement and dFC	Time-averaged measures of salience network–centered cross-network interactions were significantly lower in children with ADHD compared with typically developing children and were correlated with severity of inattention symptoms Children with ADHD displayed more variable dynamic cross-network interaction patterns, including less persistent brain states, significantly shorter mean lifetimes of brain states, and intermittently weaker cross-network interactions Dynamic time-varying measures of cross-network interactions were more strongly correlated with inattention symptoms than with time-averaged measures of FC
Autism spectrum disorder (ASD)	[41] rs-fMRI 45 ASD+ADHD patients 45 ASD-only patients 45 healthy controls	Group ICA	ASD+ADHD group had aberrant intra-network DMN connectivity, lower connectivity than control group ASD-only group had higher connectivity than control

Table 2. Continued.

Cognitive phenomenon/condition	Source, task paradigm, modality, cohort/review size	Computational approach and connectivity analysis	Reported network interactions
	[42] rs-fMRI 28 male children with ASD (15 exercise group, 13 control group)	Dynamic ICA	Identified two networks involved with cross-network 3NM connectivity and dynamic alterations in the DMN
	[43] rs-fMRI 44 ASD+ADHD patients 60 ASD-only patients 35 ADHD-only patients 81 healthy controls	Spectral DCM	Groups exhibited both shared and disorder-specific EC alterations within 3NM
	[44] Behavioural measures of social cognition compared to rs-fMRI 24 youth with ASD 25 youth with early-onset psychosis (EOP) 26 age-matched typically developing controls	Seed-based FC analysis	ASD patients had aberrant connectivity in the DMN, CEN overconnectivity and SN underconnectivity EOP patients had DMN and CEN overconnectivity
Substance use disorder (SUD) such as alcohol use disorder (AUD), cocaine use disorder (CUD), tobacco use disorder (TUD)	[35] rs-fMRI 54 cocaine user participants 54 age- and sex-matched healthy controls	Graph theory based community detection	Characterized 3NM based state dynamics by quantifying occurrence rate and transition probabilities, correlating to cocaine dependence severity Confirms DMN hyperactivity and SN dysfunction in in CUD
	[36] rs-fMRI during visual fixation 76 heavy alcohol drinker participants	Seed-based connectivity clusters for FC	FC within the CEN was significantly associated with AUD symptoms
	[37] rs-fMRI 69 patients (41 males, 28 females) stratified into heavy, moderate and non-users of alcohol	Seed-based connectivity analysis and multivariate pattern analysis	Heavy users demonstrated reduced connectivity between the superior lateral occipital cortex and the precuneus, and hypoconnectivity between the orbitofrontal cortex and language-related regions.
	[38] Smoking-related clinical scales compared to rs-fMRI 87 male TUD patients 45 male healthy control	Group ICA, sliding window and k-means clustering	TUD patients had increased static connectivity between SN and ECN, connectivity positively correlated with Russell Reasons for Smoking Questionnaire IV-VII scores
Post-traumatic stress disorder (PTSD)	[45] rs-fMRI 27 PTSD patients 33 trauma-exposed controls 30 healthy controls without trauma	ICA and DCM for EC	Enhanced ECN positive connectivity from left posterior parietal cortex to left dorsolateral prefrontal cortex was correlated with intrusion symptoms and showed good performance in detecting PTSD patients Decreased causal flow observed in SN from right amygdala to right insula and a lower transit value for the right amygdala in PTSD patients relative to trauma-exposed controls

Table 2. Continued.

Cognitive phenomenon/condition	Source, task paradigm, modality, cohort/review size	Computational approach and connectivity analysis	Reported network interactions
	[46] rs-fMRI 91 women (28 healthy control, 19 conventional PTSD, 18 PTSD dissociative subtype, 26 dissociative identity disorder)	ICA and dual regression approach for subject-specific network maps	Dissociation subtypes have robust FC signatures Dissociation linked to hyperconnectivity within 3NM, and decreased connectivity of CEN and SN with other areas
	[47] Review for PTSD art therapy using multiple modalities 19 studies (5 MRI, 5 functional near-infrared spectroscopy, 4 EEG, 2 heart rate variability, 5 other biomarker studies)	Narrative synthesis of empirical research on neurophysiological effects of art therapy	Proposes framework based on 3NM to consider network-based dysfunctions due to PTSD
Alzheimer's Disease (AZD) and Parkinson's Disease (PKD), including Mild Cognitive Impairment (MCI)	[48] rs-fMRI 17 cognitively normal participants with a family history of AZD and at least one copy of the apolipoprotein e4 allele 12 individuals	ICA and Bayesian network for inter- and intra-FC and EC	Allele carriers demonstrated aberrant within-network FC, and preserved between-network EC
	[49] rs-fMRI 30 AZD patients 14 amnestic mild cognitive impairment patients 18 healthy controls	Voxel-mirrored homotopic connectivity for aberrant connectivity analysis	Significant interhemispheric connectivity found throughout 3NM AZD patients exhibited lower connectivity values
	[50] rs-fMRI 33 AZD patients 24 late MCI patients 25 age- and sex- matched healthy controls	Seed-based FC	SN-centered interactions are impaired in patients
	[51] rs-fMRI 41 PKD patients with depression 64 PKD patients without depression 55 healthy controls (HCs)	ICA for inter- and intra-network FC	PKD patients exhibited abnormal FC values within 3NM PKD patients demonstrated decreased connectivity between anterior SN and bilateral ECN, between posterior SN and dorsal DMN, and between precuneus and dDMN/SMN/ bilateral ECN Connectivity within the left hippocampus of dorsal DMN and the right medial superior frontal gyrus of anterior SN is a significant predictor of depression level in PKD patients

Table 2. Continued.

Cognitive phenomenon/condition	Source, task paradigm, modality, cohort/review size	Computational approach and connectivity analysis	Reported network interactions
	[15] Episodic memory, executive functioning tasks compared to rs-fMRI 44 subjective cognitive decline 49 amnestic mild cognitive impairment 58 healthy control	Correlation analysis and logistic regression analysis for dFC	Non-healthy subjects had altered variability in DFC within CEN Altered variability a biomarker for preclinical Alzheimer's spectrum disorders
	[16] Mini-Mental State Examination assessment compared to rs-fMRI 53 early MCI patients 38 late MCI patients 34 healthy elderlies	ICA and expert-labelled dual-regression analysis	Longer dwell times, increased brain state transitions and deteriorated network stability in MCI patients
	[52] rs-fMRI 40 subjective cognitive decline patients 45 healthy controls	Dynamic amplitude of low-frequency fluctuation for dFC	Decreased local dynamic connectivity in FPN with compensatory visual efforts and bottom-up attention
	[53] Glucose metabolism in AZD using PET/MRI 21 AZD patients 21 MCI patients 24 healthy controls	Random-walk based community detection and network segregation analysis	AZD patients showed reduced segregation in 3NM, associated with cognitive impairments Healthy controls demonstrated SN segregation coupled with glucose metabolism
	[55] rs-fMRI 33 AZD patients 39 healthy controls	Energy landscape analysis	AZD patients had unstable and aberrant activity patterns, with high frequency in transition states
	[71] rs-fMRI and PET 128 amnestic MCI patients	Network segregation metrics	Tau pathology contributes to mild behaviour impairment by disrupting SN function
	[56] rs-fMRI 30 AZD patients 30 healthy controls	Energy landscape analysis	AZD patients had higher occurrence frequency and transition frequency between cognitive control and sensory integration brain states
	[54] Individual alpha frequency transcranial alternating stimulation and MEG recordings (2 pre-, 1 post-stim) 27 healthy participants	Leakage corrected amplitude envelope correlation for dFC and sFC	IAF-tCAS reduces sFC across DMN
	[17] rs-fMRI 761 MCI patients 1236 healthy controls	Multivariate source-based morphometry	MCI patients had lower connectivity, logistic regression showed significant association of SN connectivity with MCI

Table 2. Continued.

Cognitive phenomenon/condition	Source, task paradigm, modality, cohort/review size	Computational approach and connectivity analysis	Reported network interactions
Pain	[57] Chronic migraine self-reporting compared to rs-fMRI 25 patients 25 healthy controls	Region-of-interest to region-of-interest between 8 networks and 15 subcortical areas	Patients had increased FC between SN, sensorimotor network and DAN; between nucleus accumbens and DMN; within DMN; between thalamus and DAN Decreased FC between nucleus accumbens and DAN; within DAN Higher depression scale score positively correlated with increased intra-DMN FC
	[58] Menstrual pain compared to rs-fMRI 100 female participants	ICA for identifying resting state FC networks	Menstrual pain severity positively associated with FC between the cingulo-opercular SN and sensory processing regions, limbic regions, and insula; cSN positively associated with left CEN Menstrual pain interference is positively associated with connectivity between the cSN and widespread brain areas. Menstrual pain interference positively associated within left CEN Cumulative menstrual pain exposure shared strong negative association with FC between the DMN and widespread regions
	[59] Temporomandibular disorders using rs-fMRI	Narrative review of 3NM	Patients with temporomandibular disorders have abnormal activation of attention-related brain regions in the DMN (possibly linked to pain rumination) Decreased activity and metabolism seen in CEN pain regulation regions, abnormal activation in regions associated with negative emotions SN showed aberrant activation and metabolic changes in pain perception regions
	[60] Longitudinal study of rs-fMRI associated with social pain 93 typically developed youth (47 females, 46 males)	Yeo-7 network atlas parcellation with average Pearson correlation coefficient between pairs of networks	Social pain network exhibits substantial overlap with SN (dACC and anterior insula) but includes subgenual ACC which SN does not No observed longitudinal changes in connectivity between the FPN and DMN
Traumatic brain injury (TBI)	[61] rs-fMRI 109 acute TBI patients (61 males, 48 females) 41 chronic TBI patients (23 males, 18 females) 65 matched healthy controls (29 males, 36 females)	ICA and network interaction index for dFC with comparison to sFC	TBI patients had significantly increased and more variable dynamic cross-network interactions Increased cross-network interactions implied more severer and multiple domains of cognitive impairment

Table 2. Continued.

Cognitive phenomenon/condition	Source, task paradigm, modality, cohort/review size	Computational approach and connectivity analysis	Reported network interactions
	[62] rs-fMRI 45 acute TBI patients 40 healthy controls	ICA based resting state network FC compared to cognitive test performance	Mild TBI patients had increased FC between SN (left insula) and ECN (left superior parietal gyrus) Decreased FC within DMN (between left superior frontal gyrus and left angular gyrus) SN and DMN inter-FC showed subregion coupling increases and decreases
	[63] rs-fMRI 30 acute TBI 30 healthy controls	ICA with sliding time window correlation and k-means clustering for dFC compared to clinical variables	Dynamic FC of 3NM clustered into 5 different brain states, with patients spending longer in states characterized by weakened dorsal DMN and anterior SN inter-FC; and positive correlation between DMN and SN intra-FC
Disorders of consciousness (DOC)	[64] rs-fMRI 25 vegetative-state/ unresponsive wakefulness syndrome patients 14 minimally conscious state patients 30 healthy controls	Region-of-interest FC and fractional amplitude of low-frequency fluctuation	Vegetative state compared to minimally conscious patients showed decreased FC between DMN (PCC) and SN (left anterior insula); between SN (right anterior insula) and ECN (left dorsolateral prefrontal cortex); within SN (right anterior insula and right amygdala)
Problematic internet use (PIU)	[65] Clinical questionnaire with rs-fMRI 30 adolescents with PIU 30 healthy controls	ICA based resting state network correlations compared to clinical data	PIU patients showed higher FC between left lateral prefrontal cortex and left anterior insula Lateral prefrontal cortex showed lower intra-FC; lower inter-FC with medial prefrontal cortex and right lateral parietal cortex Left lateral and medial differences mediated by emotional symptoms
	[66] Clinical questionnaire with rs-fMRI 119 healthy participants (73 males, 46 females)	ICA based region-of-interest to region-of-interest FC analysis	Increase in FC between DMN and FPN contributes to beneficial mind wandering and may support cognitive performance

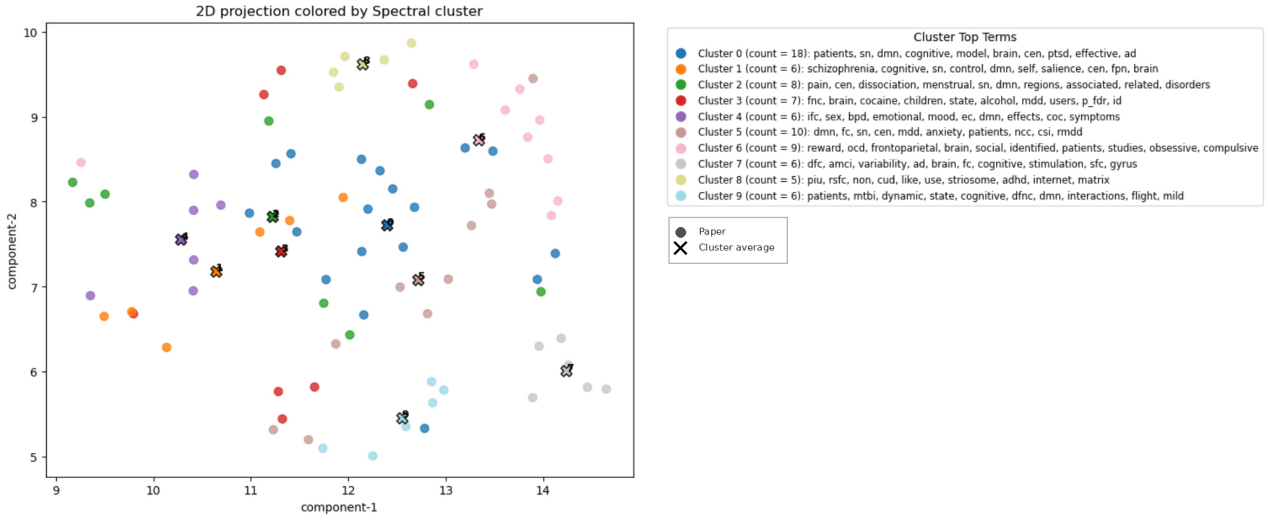

Fig. 8. Spectral clustering of paper abstracts grouped into themes. Using the eigenvector spectrum of the similarity matrix representing all encoded abstracts compared to each other, a dimension reduction can be done and clustering performed in that latent space. Coloured circles represent papers in a common cluster, and coloured diagonal crosses represent the average point of those clusters.

rimotor complex in healthy humans, and has been used to characterise synergetic configurations and synchronization stability of SN regions for those with ASD [160,161,162]. Dysfunction in SN subregions such as the insula has been associated with severity of symptoms and aberrant internetwork connectivity in major depressive disorder (MDD) [163], SUD [164], psychosis risk [70], and mild behavioural impairment [71].

2.7 Control-Theoretic Reframing

Control theory is a powerful theoretical framework for analyzing complex processes. It has been applied to neuroscience [165,166], proposing models at different levels of cognition such as interoception [167], motor control [168], and speech [169]. Importantly, optimal feedback control [170] presents both an explanatory model for embodied biological processes and a framework for designing artificial systems. This broad engineering approach [171,172] to understanding biological systems has led to the design of neuromorphic systems [173] that incorporate principles from both control theory and neuroscience [132]. Brain network control theory [174,175,176] is a promising avenue for understanding the complex brain dynamics as optimal control across the spatial connectome. We now consider the implications for the 3NM.

Coordinate-based meta-analysis techniques such as activation likelihood estimation (ALE) provide a way to test different neuroimaging studies and consistency of foci activation across experiments. We propose that a control-theoretic reframing of source activation analysis using the space of symmetric positive-definite (SPD) matrices provides a more comprehensive account because it considers the global relationship of signals as a single point (matrix) [177]. These matrices typically arise from the covariance structure of a signal. The windowed processing of covariances forms a discrete ordered set of SPD matrices representing a trajectory over time. When the set of SPD matrices is imposed with a particular metric then a particular Riemannian geometry over the set of points is prescribed, defining a topological manifold [178]. The combination of a space of representations for brain signal covariances over time and a geometry under which a trajectory must adhere provides a robust space for analyzing multi-channel data in a SPD state space. Applications in EEG [179] are relatively new, and have shown some success in brain-computer interfaces (BCI) [180,181] including the development of biomarkers [182]. SPDs also arise in a specialized form of MRI processing called diffusion tensor imaging (DTI) [183] where finding optimal paths, known as geodesics [184], are estimated in white matter [177]. Importantly, they have been used in the study of FC [185,186,187] from neuroimaging data where the space of SPD covariance or correlation matrices is embedded into a low dimensional curved surface called manifold learning [188].

This geometric approach has gained recent traction in the literature, with several studies exploring the implications of manifolds for understanding brain function and connectivity [189]. Recent work has implemented manifold learning to characterize both resting state and attention-based FC [190] from time-evolving brain state changes using fMRI. Manifold learning has been used on rs-fMRI to predict age and demonstrated integration and segregation of cortical-subcortical networks across lifespan [191]. More traditional Riemannian geometry has also been used with FC to harmonize data across multiple sites collecting neu-

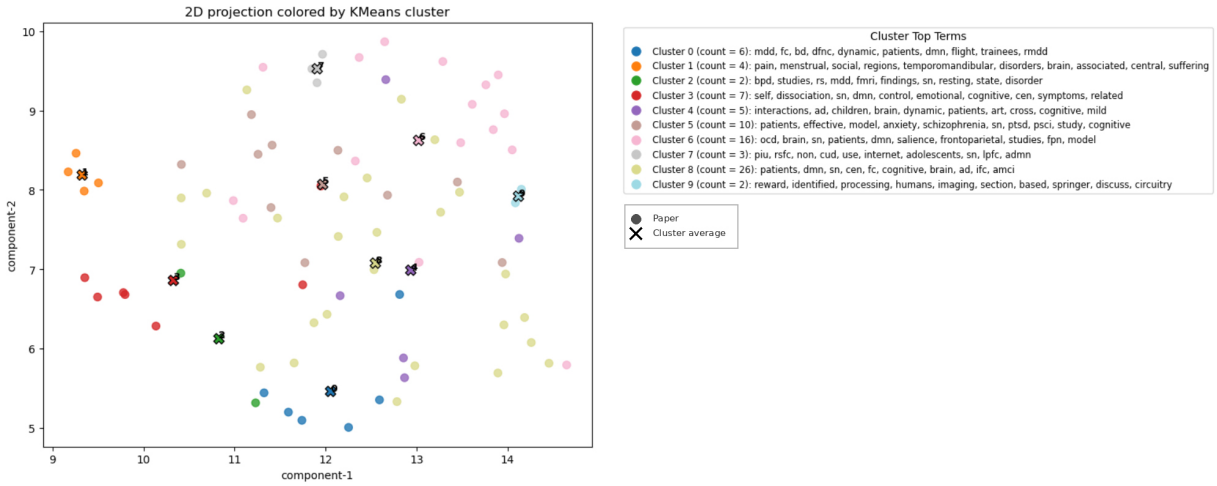

Fig. 9. K-means clustering of paper abstracts grouped into themes. Using the raw distributional semantic vectors from the paper abstracts and pre-determining a number of clusters (fine-tuned based on other clustering results), a Euclidean distance based clustering can be done by grouping papers based on a center of mass. Coloured circles represent papers in a common cluster, and coloured diagonal crosses represent the average point of those clusters.

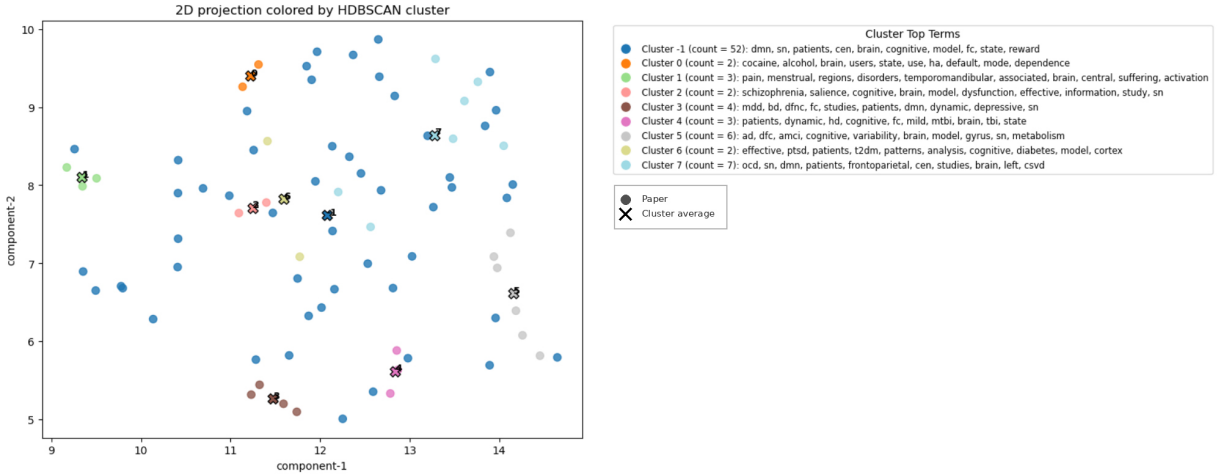

Fig. 10. HDBSCAN clustering of paper abstracts grouped into themes with a noise cluster. HDBSCAN automatically determines the number of clusters based on a radius parameter for grouping, and identifies an outlier class of points that do not fit well into any identified clusters. HDBSCAN, hierarchical density-based spatial clustering of applications with noise. Coloured circles represent papers in a common cluster, and coloured diagonal crosses represent the average point of those clusters.

roimaging data related to ADHD [192]. This geometric approach has been applied to the meso-scale to characterize the relationship between neural circuits and their manifold representations [193,194]. This has been further extended using a geometric deep learning approach for interpretable representations of neural population dynamics [195]. Interestingly, motor behaviours have been shown to be encoded within these neural manifolds [196,197] as well as perceptual processes [198]. It has also been applied to decoding brain states during wakefulness and sleep [199]. The optimal coding of tasks on neural manifolds at the neural population level is an active area of research [200].

In low dimensions, the space of SPD matrices may be represented as the interior of a cone. This means that all possible SPD matrices have an associated point inside the cone (and vice-versa). By expressing brain region covariances as SPD matrices, we may effectively embed the state of possible brain states into this cone. Cognitive transitions may thus be described as the paths or trajectories between these points over time. Datasets across subjects and paradigms may be represented as clusters of points in this cone. When considering that the matrices are points living in the cone, Riemannian geometry allows for the calculation of distances between points without leaving this

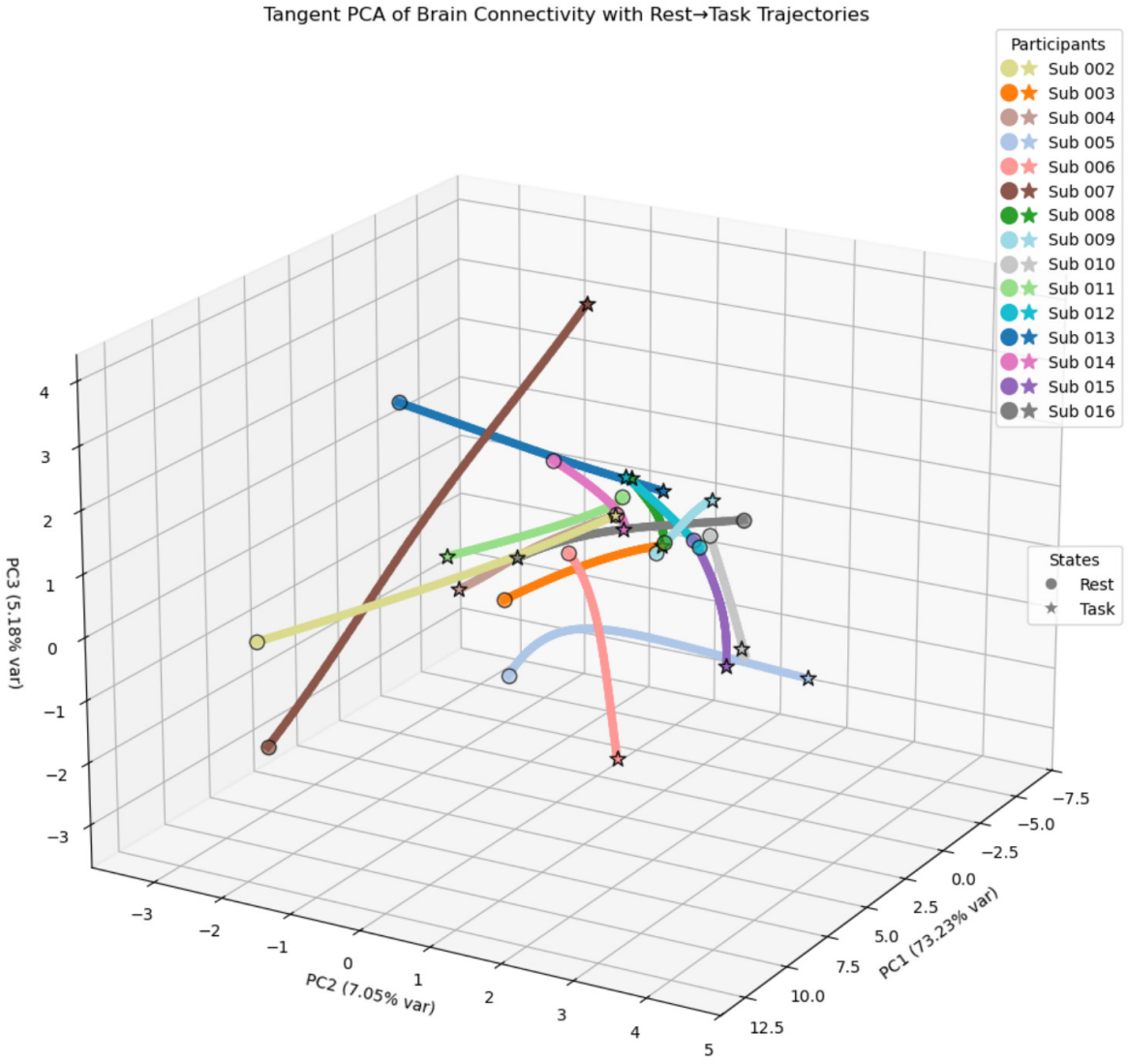

Fig. 11. Tangent PCA of [68]. Given two sets of source localized region averaged time series for rest and task states, a sliding one second window dFC analysis is used to compute a series of AIM-based SPD matrices. The Karcher mean of each time series is then computed, and the geodesic between these two averages plotted in the first three tangent PCA component space. Axes represent top three principal components and their eigenvalues reported as percentage of total variance. Different colours represent different subjects, and different shapes (star/circle) represent Karcher means for different stimuli conditions. This empirically visualizes the optimal path of brain region covariances between resting and task state in a truncated subspace. For two conditions, this means the start and endpoint of each curve represents the average SPD matrix for the respective rest/task state from recorded data. PCA, principal component analysis; dFC, dynamic functional connectivity; AIM, affine-invariant metric.

cone, while Euclidean geometry may produce a path that crosses the cone boundary (and thus outside of the space of valid brain signal covariances). Fig. 4 demonstrates this low-dimensional example. Two points in the cone may be connected by a path that remains in the cone and respects the geometry of the space (which can be thought of as densities in the space which the path must navigate around). By adopting Riemannian geometry, comparisons between covariance configurations of brain signals remain valid when describing transitionary states.

In order to elucidate the implications of Riemannian geometry to the 3NM, we highlight the necessary ingredients: (i) Defining an SPD covariance manifold, modality-dependent and derived from an appropriate atlas-based parcellation of multichannel signals, either spatially sparse like EEG or region-based averaged from source localized or volumetric data; and (ii) finding a geometry imposed by the selection of a metric, which themselves form a manifold of metrics [201]. The SPD spaces induced by a sparse set of raw EEG signals, or by source localized and atlas-

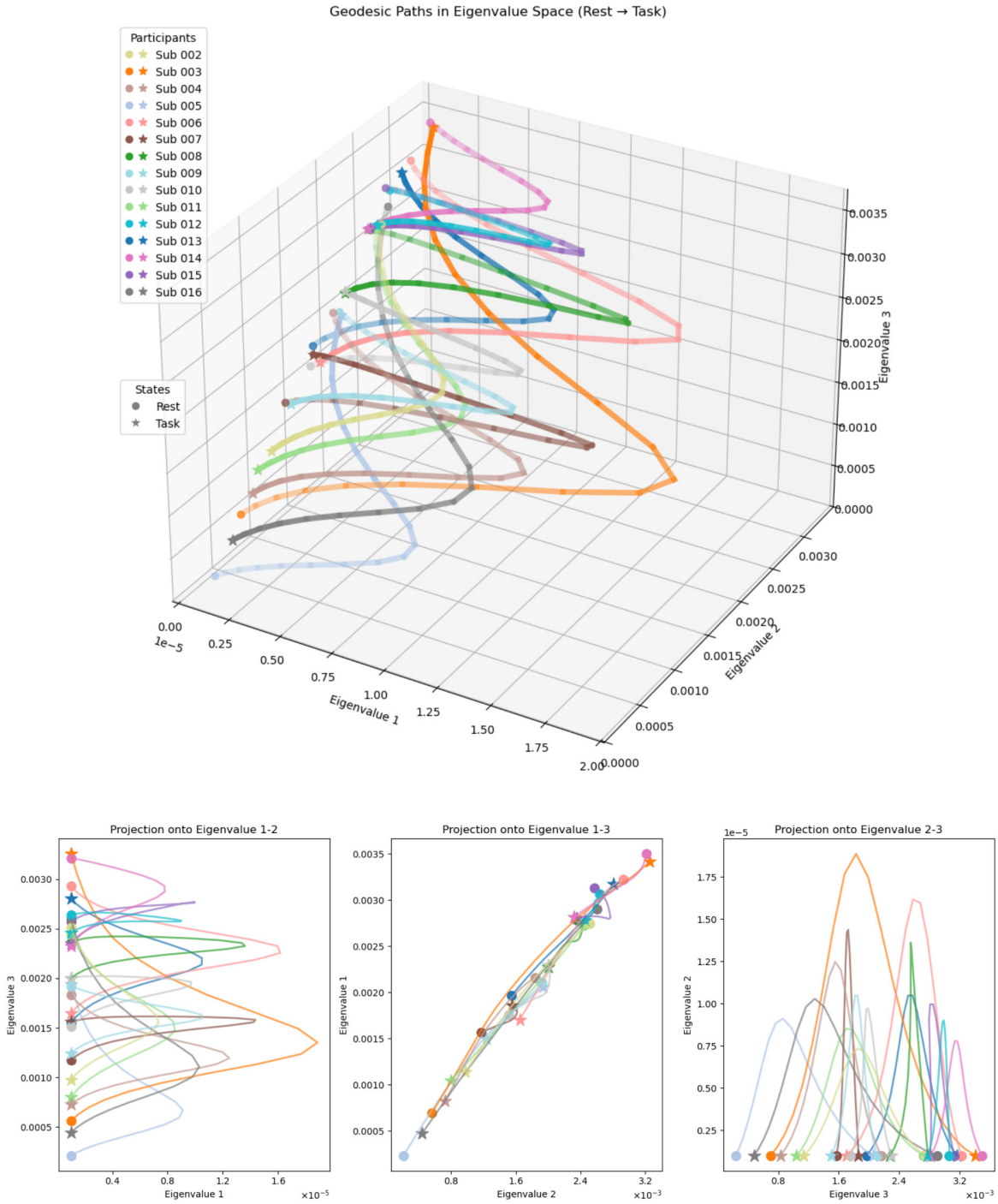

Fig. 12. Eigendecomposition of SPD matrices from [68]. The dFC matrices for rest and task were eigendecomposed and the first three values plotted. The lines between rest and task points represent the weight changes in the eigenvalues along the optimal geodesic between them. This thus provides a more detailed landscape of trajectories on which transitional brain states can be compared against.

based averaging, or by volumetric imaging techniques such as fMRI are all different (in the sense of their underlying generating processes). Indeed, the SPD spaces of two sets of EEG recordings with different surface atlases will be different. This, however, does not mean they are incompatible. Source localized data and volumetric imaging may be compared after a normalization into a common parcellation such as HCPex to generate two SPD spaces whose trajectories may be correlated. This remains coordinate-based, but rather than considering individual region activations, the global covariance geometry is considered.

By comparing the geometry of the covariance between regions across modalities, the underlying mechanisms may be identified given that one SPD geometry

would be driven by the magnetoelectrophysiology of the source localized data and the other SPD geometry is driven by the neurophysiology of the volumetric imaging modality, e.g., BOLD signals in fMRI. The choice of metric defines and determines the geometry of the space [202]. Four metrics emerge, each with their consequences for interpretability: affine-invariant metric (AIM), log-Euclidean metric (LEM), log-Cholesky metric (LCM), and Bures-Wasserstein metric (BWM). Each has their advantages and disadvantages regarding preservation of useful mathematical properties as well as practical considerations regarding computational efficiency. AIM, equivalent to the Fisher-Rao metric for Gaussian covariances, ensures full invariance under affine transformations, preserving statistical meaning in brain signal covariances. It maintains geodesic convexity for means, though matrix inversions raise computational costs. LEM embeds SPD matrices into Euclidean space via matrix logarithms, enabling fast vector-space operations like averaging for real-time EEG processing. It is computationally efficient to compute and therefore possibly suitable for real-time applications, but sacrifices full affine invariance, potentially distorting anisotropic brain connectivities. LCM uses Cholesky decomposition to linearize SPD matrices, balancing invariance with numerical stability for high-dimensional data such as fMRI. It supports efficient optimization in brain network regression but introduces approximation errors in non-cartesian geometries, limiting interpretability of phase-amplitude couplings in oscillatory EEG. BWM aligns with optimal transport, ideal for fusing multimodal neuroimaging (e.g., EEG-fMRI covariances) due to its symmetric metric property on distributions. It aids generative modeling of functional networks but demands costly singular value decompositions, hindering scalability for large-scale brain analysis.

Using Riemannian geometry, hypotheses about the 3NM can be tested by implementing geodesic clustering [203] and principal geodesic analysis (PGA) [184] of the space, generalizations of regular Euclidean space clustering and principal component analysis (PCA) but respecting the imposed geometry. Geodesic distances on regularized functional connectomes have been used for precision characterization of neural activity at the individual level [204]. Clustering based on this geometry-aware distance between points, has been applied to time-series for network-wide brain analysis based on GC [205]. A statistical dimensionality reduction to explain variability in geodesic distances, probabilistic PGA using MRI data analyzed shape variability in the corpus callosum across individuals [206]. This approach provides a rigorous treatment of intrinsic statistics for Riemannian geometry such as the Fréchet mean, sometimes called the Karcher mean or Riemannian barycenter representing a geometric generalization of an average. This matrix is the center of mass for a set of matrices, determined by minimizing the geodesics for all points simultaneously [207].

A demonstrative example using a preprocessed input dataset from a reviewed paper is available in the Appendix Figs. 11,12 (Ref. [68]). Using AIM and the Karcher mean of the dFC time series for both rest and task matrices, a geodesic between these two SPD points per subject was computed representing the optimal path of brain region covariances between states as observed in recorded data. The rest/task Karcher means represent the matrices that minimize the geodesic distance to all observed time window covariance matrices for each experimental phase respectively. This represents a landscape of possible trajectories between brain states that may be perturbed. The original analysis presented a neural mass and masking-based model of the 3NM that identified SN-driven facilitation of both DMN and TPN during recall, stronger TPN–DMN inhibition during rest, and a reversal in DMN-to-SN influence across states. The 3NM nodes used a HCP-MMP atlas, and the constituent regions for each of the SN, DMN and TPN can be found in the supplementary material of the report from which the dataset was taken [68]. Notably, the DMN included the PCC, the TPN included the dorsolateral prefrontal cortex, and the SN included the insular and frontal opercular cortex. In order to validate such network labellings and connectivity results, methods such as system identification [208] can be applied to the Riemannian manifold representations of the dFC signals. Recent approaches include modern convolutional [209] and recurrent [210] neural networks. This reframes proposed connectivities as hypotheses that can be tested by estimating/recovering a dynamical system from the data and comparing interactions between regions. Furthermore, these approaches may benefit from the existing work done in general for system identification [211].

We now present a conceptual interpretation of the 3NM and the macro-scale functional network parcellations [5] as control-theoretic dynamical systems. We assume a simplified sensor-control-action loop and that perception (both intero- and extero-) as well as action are bodily and environmentally bounded control processes. Fig. 5 demonstrates how the 3NM may be described as closing such an embodied loop. Fig. 6 (Ref. [5]) demonstrates the six networks suggested by the macro-scale taxonomy. Here, the difference between the number of constituent networks is important. The number of possible configurations for a possibly bidirectional graph with n nodes is $4^{n(n-1)/2}$, given four possible edge states (i.e., no connection, either of the one-way connections, or a bidirectional connection) and the number of possible edges. For the space of possible 3NM graph configurations, from a model assuming no connectivity to a model assuming full bidirectional connectivity, there are only 64 possible configurations. For a six network model, this becomes over one billion; Fig. 6 is a speculative hypothetical configuration amongst many. This suggests the parcellation of large-scale networks and their interpretability should remain low as to not explode in com-

binatorial possibilities, but not so low as to lack the expressivity of different roles and relationships between them that may be tested by neuroimaging data.

Consider the 3NM interpretation towards a control-theoretic frame with testable SPD approaches: (i) DMN dynamics are a set of meta-stable attractors such as between rest and task, (ii) SN modulation is an error-correcting signal from regions involved with integrating perception and attention, (iii) CEN heterogeneity is a parallel set of anatomically separate regions weighted by modulation. Conceptually, different reported activity of DMN-labeled regions for resting state and multiple task paradigms may be interpreted as bistable or multi-stable attractors. Phenomena such as mind-wandering may be described as a drifting trajectory on the manifold with an underlying salience mechanism. Cognitive disorders caused by biophysiological effects such as TBI or PTSD may be described as geometric deformations. Mathematically, such deformations can be considered as stretching or shrinking geodesics, and thus increasing or decreasing the control energy needed to transition between states. Attractor stability is facilitated by SN regions integrating and filtering sensory information in order to propagate a modulatory signal to DMN and CEN related regions. Attention-related disorders may be described as perturbations to this dynamic equilibrium. Finally, network-of-network descriptions of connectomes may be described by submanifolds. CEN heterogeneity is thus the collective action of parallel submanifolds weighted in their contribution by the modulating SN signal. This allows for a context-dependent account of specialized processing regions associated with the CEN.

Following the more anatomically grounded macroscale functional network taxonomy [5], the six identified networks (ON, PN, D-FPN, L-FPN, M-CIN, M-FPN) may also be control-theoretically reframed. Sensory and perceptual processing in the occipital network acts as a sensory input boundary where stimuli is represented as high-dimensional exogenous information. The pericentral network serves as the embodied feedback loop based on motor-sensory coupling between the PN and ON. The dorsal and lateral frontoparietal networks both contribute to goal-directed attention, working memory and cognitive control. The midcingulo-insular network integrates signals from the ON and PN and generates an error-correcting signal across other networks, modulating their activity. The medial frontoparietal network serves as a driving default mode signal, modulated in a graded relationship with the D/L-FPNs.

3. Conclusions

Despite differences in labeling and methodology, the studies reviewed here converge on several key principles. First, control networks act as flexible hubs, biasing or suppressing activity in both processing and default networks. Evidence from EEG–fMRI studies shows that frontal theta activity is negatively correlated with DMN hubs [12], while fMRI-based analyses highlight the frontoparietal network's modulation of alpha-band activity in visual association cortices [6]. More recently, intracranial EEG has demonstrated directed influence of the anterior insula on both DMN and CEN activity during memory tasks [69]. Together, these findings underscore the modulatory role of control networks in coordinating distributed brain systems.

Apparent disagreements across studies are often attributable to differences in anatomical labeling rather than fundamental functional discrepancies. The same cortical region may be assigned to different networks depending on the atlas (e.g., HCP vs. DK) or the modality used (e.g., BOLD-based connectivity vs. oscillatory source reconstruction). Reconciling these inconsistencies requires frameworks that integrate across scales and methods. Multimodal approaches, which combine the temporal precision of EEG with the spatial specificity of fMRI, are particularly well positioned to advance this goal.

Several gaps remain. One concerns the temporal dimension of network function, which has received less emphasis in current taxonomies. Although temporality is often acknowledged indirectly—through descriptions of modulatory interactions—the explicit incorporation of oscillatory and state-dependent dynamics into network definitions may provide a more complete account of large-scale organization. Another gap concerns individual variability: large-cohort studies highlight substantial heterogeneity in connectivity profiles [79], raising the question of whether spectral "fingerprints" of networks are stable traits or context-dependent states. Furthermore, some practical challenges of multimodal precision models remain. Most brain atlases are based on population-level averages and therefore network conclusions from such parcellations may not accurately reflect individual biology. Although this may be improved by incorporating the spatial information available in volumetric signals and taking long-running recordings, precision brain mapping remains an open problem ameliorated by imaging data fusion.

Additionally, we identify a need for more sophisticated modelling approaches that can account for the multiplicity of brain states and their transitions over time as observed in the 3NM disorder literature. Specifically, no studies to date have systematically characterized the temporal dynamics of network interactions in 3NM disorders using a control-theoretic perspective. Appendix Table 2 may thus serve as a useful map for researchers interested in either methodology or reported 3NM findings. The diversity of our reported review shows that without such an approach, important aspects of network function across temporal and spatial scales may be overlooked. Furthermore, the neural manifold reframing allows seemingly conflicting results reporting hyper- and hypo-connectivity within the same networks across disorders, such as the DMN in schizophrenia and CEN in ADHD, as different subregions or deformations of the same manifold. Phenomena such as com-

pensatory recruitment can be interpreted as occupying the manifold region where coupling is high as a result of cognitive load, and structural degradation can be interpreted as the manifold region with lower coupling as a result of neuropathological biophysics. Although such interpretations are not yet settled, the manifold approach provides a representative basis capable of describing both neurotypical and disordered cognitive brain states without committing to a specific latent explanatory cause.

As an addendum to the existing suggestions in the literature [143,212,213], we thus propose the following guidelines: (i) imaging modalities should be selected based on the specific research question and the temporal and spatial resolution required, (ii) multimodal approaches should be prioritized to leverage the strengths of different imaging techniques, and (iii) network analysis should go beyond FC/EC and include analyses of oscillatory dynamics, state transitions, and temporal variability. Fig. 7 presents a proposed decision workflow for connectivity analysis that combines these guidelines into specific and actionable research design.

Future work may benefit from integrating covariance structures of oscillatory dynamics with connectivity-based parcellations, moving toward a taxonomy that captures not only spatial and functional specificity but also temporal dynamics grounded in anatomical labellings. Such an approach could help resolve ongoing controversies in network labeling, provide a richer account of cognitive control, and better inform models of psychopathology. All in all, the usefulness of taxonomies, atlases and other anatomical graphical representations partly resides in capturing the possible *in vivo* functional dynamics. Emerging geometrical approaches, such as the one we have sketched out, might eventually lead to representational advances which might help rethink structural networks as configurations of brain activity, rather than simply as static real estates, and encourage the inclusion of timescale information when interpreting functional configurations (networks).

Availability of Data and Materials

The raw data of survey abstracts is accessible using the built-in export functions on both Scopus and PubMed using the query described in the paper. All data reported in this paper will also be shared by the lead contact upon request.

Author Contributions

MP designed the research study, performed the main analysis and wrote the manuscript. SO performed an initial manual mini-survey to determine a useful search query across databases. HP contributed to the data analysis and subsequent manual citation search and review. RC and AD'A acquired funding, conceive and design the study, contributed to drafting the work and reviewed important revisions and content. All authors contributed to editorial changes in the manuscript. All authors read and approved the final manuscript. All authors have participated sufficiently in the work and have agreed to be accountable for all aspects of the work.

Ethics Approval and Consent to Participate

Not applicable.

Acknowledgment

We thank Maryam Mehri Dehnavi.

Funding

This research was supported by a New Frontiers in Research Fund Exploration grant (NFRFE -2019-00503).

Conflicts of Interest

Given his role as the Guest Editor member, Amedeo D'Angiulli had no involvement in the peer review of this article and has no access to information regarding its peer review. Full responsibility for the editorial process for this article was delegated to Bettina Platt.

Declaration of AI and AI-Assisted Technologies in the Writing Process

During the preparation of this work the authors used Claude Haiku 4.5 in order to check spelling and grammar. After using this tool, the authors reviewed and edited the content as needed and take full responsibility for the content of the publication.

Appendix

See Figs. 8,9,10,11,12 and Tables 1,2.

References

[1] Menon V. Large-scale brain networks and psychopathology: a unifying triple network model. Trends in Cognitive Sciences. 2011; 15: 483–506. https://doi.org/10.1016/j.tics.2011.08.003

[2] Menon B. Towards a new model of understanding - The triple network, psychopathology and the structure of the mind. Medical Hypotheses. 2019; 133: 109385. https://doi.org/10.1016/j.mehy.2019.109385

[3] Spreng RN. The fallacy of a "task-negative" network. Frontiers in Psychology. 2012; 3: 145. https://doi.org/10.3389/fpsyg.2012.00145

[4] Fox KCR, Spreng RN, Ellamil M, Andrews-Hanna JR, Christoff K. The wandering brain: meta-analysis of functional neuroimaging studies of mind-wandering and related spontaneous thought processes. NeuroImage. 2015; 111: 611–621. https://doi.org/10.1016/j.neuroimage.2015.02.039

[5] Uddin LQ, Yeo BTT, Spreng RN. Towards a Universal Taxonomy of Macro-scale Functional Human Brain Networks. Brain Topography. 2019; 32: 926–942. https://doi.org/10.1007/s10548-019-00744-6

[6] Marek S, Dosenbach NUF. The frontoparietal network: function, electrophysiology, and importance of individual precision mapping. Dialogues in Clinical Neuroscience. 2018; 20: 133–140. https://doi.org/10.31887/DCNS.2018.20.2/smarek

[7] Glasser MF, Coalson TS, Robinson EC, Hacker CD, Harwell J, Yacoub E, et al. A multi-modal parcellation of human cerebral cortex. Nature. 2016; 536: 171–178. https://doi.org/10.1038/nature18933
[8] Desikan RS, Ségonne F, Fischl B, Quinn BT, Dickerson BC, Blacker D, et al. An automated labeling system for subdividing the human cerebral cortex on MRI scans into gyral based regions of interest. NeuroImage. 2006; 31: 968–980. https://doi.org/10.1016/j.neuroimage.2006.01.021
[9] Huang CC, Rolls ET, Feng J, Lin CP. An extended Human Connectome Project multimodal parcellation atlas of the human cortex and subcortical areas. Brain Structure & Function. 2022; 227: 763–778. https://doi.org/10.1007/s00429-021-02421-6
[10] Mazziotta J, Toga A, Evans A, Fox P, Lancaster J, Zilles K, et al. A probabilistic atlas and reference system for the human brain: International Consortium for Brain Mapping (ICBM). Philosophical Transactions of the Royal Society of London. Series B, Biological Sciences. 2001; 356: 1293–1322. https://doi.org/10.1098/rstb.2001.0915
[11] Holmes CJ, Hoge R, Collins L, Woods R, Toga AW, Evans AC. Enhancement of MR images using registration for signal averaging. Journal of Computer Assisted Tomography. 1998; 22: 324–333. https://doi.org/10.1097/00004728-199803000-00032
[12] Scheeringa R, Bastiaansen MCM, Petersson KM, Oostenveld R, Norris DG, Hagoort P. Frontal theta EEG activity correlates negatively with the default mode network in resting state. International Journal of Psychophysiology : Official Journal of the International Organization of Psychophysiology. 2008; 67: 242–251. https://doi.org/10.1016/j.ijpsycho.2007.05.017
[13] Britton JW, Frey LC, Hopp JL, Korb P, Koubeissi MZ, Lievens WE, et al. Electroencephalography (EEG): An introductory text and atlas of normal and abnormal findings in adults, children, and infants. American Epilepsy Society: Chicago. 2016.
[14] Ojeda A, Wagner M, Maric V, Ramanathan D, Mishra J. EEG source derived salience network coupling supports real-world attention switching. Neuropsychologia. 2023; 178: 108445. https://doi.org/10.1016/j.neuropsychologia.2022.108445
[15] Xue C, Qi W, Yuan Q, Hu G, Ge H, Rao J, et al. Disrupted Dynamic Functional Connectivity in Distinguishing Subjective Cognitive Decline and Amnestic Mild Cognitive Impairment Based on the Triple-Network Model. Frontiers in Aging Neuroscience. 2021; 13: 711009. https://doi.org/10.3389/fnagi.2021.711009
[16] Li C, Li Y, Wu J, Wu M, Peng F, Chao Q, et al. Triple Network Model-Based Analysis on Abnormal Core Brain Functional Network Dynamics in Different Stage of Amnestic Mild Cognitive Impairment. Journal of Alzheimer's Disease : JAD. 2022; 89: 519–533. https://doi.org/10.3233/JAD-220282
[17] Yotsuya C, Watanabe K, Kasai S, Umemura Y, Shintaku T, Ishimoto Y, et al. Altered connectivity among the triple brain networks in patients with mild cognitive impairment: a source-based morphometry study with a large elderly population. Japanese Journal of Radiology. 2025; 43: 1434–1444. https://doi.org/10.1007/s11604-025-01791-9
[18] Cao J, Liu G, Li X, Yue Z, Ren J, Zhu W, et al. Dynamic functional connectivity changes in the triple networks and its association with cognitive impairment in hemodialysis patients. Brain and Behavior. 2021; 11: e2314. https://doi.org/10.1002/brb3.2314
[19] Ruan Z, Zhou X, Rao B, Li Y, Sun W, Li T, et al. Network dynamics in post-stroke cognitive impairment: insights from effective connectivity analysis. Brain Imaging and Behavior. 2025; 19: 346–356. https://doi.org/10.1007/s11682-025-00972-4
[20] Doll A, Sorg C, Manoliu A, Wöller A, Meng C, Förstl H, et al. Shifted intrinsic connectivity of central executive and salience network in borderline personality disorder. Frontiers in Human Neuroscience. 2013; 7: 727. https://doi.org/10.3389/fnhum.2013.00727
[21] Shafie M, Shahmohamadi E, Cattarinussi G, Sanjari Moghaddam H, Akhondzadeh S, Sambataro F, et al. Resting-state functional magnetic resonance imaging alterations in borderline personality disorder: A systematic review. Journal of Affective Disorders. 2023; 341: 335–345. https://doi.org/10.1016/j.jad.2023.09.001
[22] Jiang Y, Duan M, Chen X, Chang X, He H, Li Y, et al. Common and distinct dysfunctional patterns contribute to triple network model in schizophrenia and depression: A preliminary study. Progress in Neuro-psychopharmacology & Biological Psychiatry. 2017; 79: 302–310. https://doi.org/10.1016/j.pnpbp.2017.07.007
[23] Kim A, Ha M, Kim T, Park S, Lho SK, Moon SY, et al. Triple-Network Dysconnectivity in Patients With First-Episode Psychosis and Individuals at Clinical High Risk for Psychosis. Psychiatry Investigation. 2022; 19: 1037–1045. https://doi.org/10.30773/pi.2022.0091
[24] Martin JC, Clark SR, Schubert KO. Towards a Neurophenomenological Understanding of Self-Disorder in Schizophrenia Spectrum Disorders: A Systematic Review and Synthesis of Anatomical, Physiological, and Neurocognitive Findings. Brain Sciences. 2023; 13: 845. https://doi.org/10.3390/brainsci13060845
[25] Menon V, Palaniyappan L, Supekar K. Integrative Brain Network and Salience Models of Psychopathology and Cognitive Dysfunction in Schizophrenia. Biological Psychiatry. 2023; 94: 108–120. https://doi.org/10.1016/j.biopsych.2022.09.029
[26] Adamczyk P, Więcławski W, Wojcik M, Frycz S, Panek B, Jáni M, et al. Aberrant information flow within resting-state triple network model in schizophrenia-An EEG effective connectivity study. Psychiatry Research. Neuroimaging. 2025; 349: 111985. https://doi.org/10.1016/j.pscychresns.2025.111985
[27] Wang J, Wang Y, Wu X, Huang H, Jia Y, Zhong S, et al. Shared and specific functional connectivity alterations in unmedicated bipolar and major depressive disorders based on the triple-network model. Brain Imaging and Behavior. 2020; 14: 186–199. https://doi.org/10.1007/s11682-018-9978-x
[28] Wang J, Wang Y, Huang H, Jia Y, Zheng S, Zhong S, et al. Abnormal dynamic functional network connectivity in unmedicated bipolar and major depressive disorders based on the triple-network model. Psychological Medicine. 2020; 50: 465–474. https://doi.org/10.1017/S003329171900028X
[29] Huang WS, Hsu JW, Cheng LK, Chen LC, Bai YM, Chen LF, et al. Triple Network Model-Based Functional Dysconnectivity in Young People With Major Affective Disorders With or Without Current Suicidal Ideation. The Journal of Clinical Psychiatry. 2025; 87: 25m15906. https://doi.org/10.4088/JCP.25m15906
[30] Kolobaric A, Andreescu C, Gerlach AR, Jašarević E, Aizenstein H, Pascoal TA, et al. Altered triple network model connectivity is associated with cognitive function and depressive symptoms in older adults. Alzheimer's & Dementia : the Journal of the Alzheimer's Association. 2025; 21: e14493. https://doi.org/10.1002/alz.14493
[31] Gürsel DA, Avram M, Sorg C, Brandl F, Koch K. Frontoparietal areas link impairments of large-scale intrinsic brain networks with aberrant fronto-striatal interactions in OCD: a meta-analysis of resting-state functional connectivity. Neuroscience and Biobehavioral Reviews. 2018; 87: 151–160. https://doi.org/10.1016/j.neubiorev.2018.01.016
[32] Gürsel DA, Reinholz L, Bremer B, Schmitz-Koep B, Franzmeier N, Avram M, et al. Frontoparietal and salience network alterations in obsessive–compulsive disorder: insights from independent component and sliding time window analyses. Journal of Psychiatry & Neuroscience : JPN. 2020; 45: 214–221.

https://doi.org/10.1503/jpn.190038
[33] Perera MPN, Gotsis ES, Bailey NW, Fitzgibbon BM, Fitzgerald PB. Exploring functional connectivity in large-scale brain networks in obsessive-compulsive disorder: a systematic review of EEG and fMRI studies. Cerebral Cortex (New York, N.Y. : 1991). 2024; 34: bhae327. https://doi.org/10.1093/cercor/bhae327
[34] Li H, Li B, Cao L, Jiang J, Chai S, Zhou H, et al. Dysregulated connectivity configuration of triple-network model in obsessive-compulsive disorder. Molecular Psychiatry. 2025; 30: 3138–3149. https://doi.org/10.1038/s41380-025-02921-5
[35] Zhai T, Gu H, Salmeron BJ, Stein EA, Yang Y. Disrupted Dynamic Interactions Between Large-Scale Brain Networks in Cocaine Users Are Associated With Dependence Severity. Biological Psychiatry. Cognitive Neuroscience and Neuroimaging. 2023; 8: 672–679. https://doi.org/10.1016/j.bpsc.2022.08.010
[36] Elsayed M, Marsden E, Hargreaves T, Syan SK, MacKillop J, Amlung M. Triple network resting-state functional connectivity patterns of alcohol heavy drinking. Alcohol and Alcoholism (Oxford, Oxfordshire). 2024; 59: agae056. https://doi.org/10.1093/alcalc/agae056
[37] Francis AN, Salloum IM. High-resolution mapping of alcohol-related brain connectivity in adults using 7T fMRI and multivoxel pattern classification. Psychiatry Research. Neuroimaging. 2025; 352: 112046. https://doi.org/10.1016/j.pscychresns.2025.112046
[38] Liu Y, Zhang M, Tian Y, Zhou S, Shen Y, Ma L, et al. Disordered connectivity configuration of triple-network model and visual-network in tobacco use disorder. Progress in Neuropsychopharmacology & Biological Psychiatry. 2026; 146: 111703. https://doi.org/10.1016/j.pnpbp.2026.111703
[39] Fan J, Zhong M, Gan J, Liu W, Niu C, Liao H, et al. Altered connectivity within and between the default mode, central executive, and salience networks in obsessive-compulsive disorder. Journal of Affective Disorders. 2017; 223: 106–114. https://doi.org/10.1016/j.jad.2017.07.041
[40] Cai W, Chen T, Szegletes L, Supekar K, Menon V. Aberrant Time-Varying Cross-Network Interactions in Children With Attention-Deficit/Hyperactivity Disorder and the Relation to Attention Deficits. Biological Psychiatry. Cognitive Neuroscience and Neuroimaging. 2018; 3: 263–273. https://doi.org/10.1016/j.bpsc.2017.10.005
[41] Wang L, Qin Y, Yang S, Jin D, Zhu Y, Li X, et al. Posterior default mode network is associated with the social performance in male children with autism spectrum disorder: A dynamic causal modeling analysis based on triple-network model. Human Brain Mapping. 2024; 45: e26750. https://doi.org/10.1002/hbm.26750
[42] Zhang W, Cai K, Xiong X, Zhu L, Sun Z, Yang S, et al. Alterations of triple network dynamic connectivity and repetitive behaviors after mini-basketball training program in children with autism spectrum disorder. Scientific Reports. 2025; 15: 2629. https://doi.org/10.1038/s41598-025-87248-5
[43] Liu H, Li C, Qin R, Li L, Yuan X, Chen B, et al. Effective connectivity alterations of the triple network model in the co-occurrence of autism spectrum disorder and attention deficit hyperactivity disorder. Cerebral Cortex (New York, N.Y. : 1991). 2025; 35: bhaf047. https://doi.org/10.1093/cercor/bhaf047
[44] Nair A, Jalal R, Lawrence KE, Verma N, Gutierrez H, Laulette K, et al. Triple-Network Functional Connectivity in Adolescents With Autism Spectrum Disorder Compared to Early-Onset Psychosis. Autism Research : Official Journal of the International Society for Autism Research. 2026; 19: e70163. https://doi.org/10.1002/aur.70163
[45] Weng Y, Qi R, Zhang L, Luo Y, Ke J, Xu Q, et al. Disturbed effective connectivity patterns in an intrinsic triple network model are associated with posttraumatic stress disorder. Neurological Sciences : Official Journal of the Italian Neurological Society and of the Italian Society of Clinical Neurophysiology. 2019; 40: 339–349. https://doi.org/10.1007/s10072-018-3638-1
[46] Lebois LAM, Kumar P, Palermo CA, Lambros AM, O'Connor L, Wolff JD, et al. Deconstructing dissociation: a triple network model of trauma-related dissociation and its subtypes. Neuropsychopharmacology : Official Publication of the American College of Neuropsychopharmacology. 2022; 47: 2261–2270. https://doi.org/10.1038/s41386-022-01468-1
[47] Malhotra B, Jones LC, Spooner H, Levy C, Kaimal G, Williamson JB. A conceptual framework for a neurophysiological basis of art therapy for PTSD. Frontiers in Human Neuroscience. 2024; 18: 1351757. https://doi.org/10.3389/fnhum.2024.1351757
[48] Wu X, Li Q, Yu X, Chen K, Fleisher AS, Guo X, et al. A Triple Network Connectivity Study of Large-Scale Brain Systems in Cognitively Normal APOE4 Carriers. Frontiers in Aging Neuroscience. 2016; 8: 231. https://doi.org/10.3389/fnagi.2016.00231
[49] Liao ZL, Tan YF, Qiu YJ, Zhu JP, Chen Y, Lin SS, et al. Interhemispheric functional connectivity for Alzheimer's disease and amnestic mild cognitive impairment based on the triple network model. Journal of Zhejiang University. Science. B. 2018; 19: 924–934. https://doi.org/10.1631/jzus.B1800381
[50] Li C, Li Y, Zheng L, Zhu X, Shao B, Fan G, et al. Abnormal Brain Network Connectivity in a Triple-Network Model of Alzheimer's Disease. Journal of Alzheimer's Disease : JAD. 2019; 69: 237–252. https://doi.org/10.3233/JAD-181097
[51] Liao H, Cai S, Shen Q, Fan J, Wang T, Zi Y, et al. Networks Are Associated With Depression in Patients With Parkinson's Disease: A Resting-State Imaging Study. Frontiers in Neuroscience. 2021; 14: 573538. https://doi.org/10.3389/fnins.2020.573538
[52] Wei YC, Kung YC, Huang WY, Lin C, Chen YL, Chen CK, et al. Functional Connectivity Dynamics Altered of the Resting Brain in Subjective Cognitive Decline. Frontiers in Aging Neuroscience. 2022; 14: 817137. https://doi.org/10.3389/fnagi.2022.817137
[53] Zhang M, Guan Z, Zhang Y, Sun W, Li W, Hu J, et al. Disrupted coupling between salience network segregation and glucose metabolism is associated with cognitive decline in Alzheimer's disease - A simultaneous resting-state FDG-PET/fMRI study. NeuroImage. Clinical. 2022; 34: 102977. https://doi.org/10.1016/j.nicl.2022.102977
[54] Carrasco-Gómez M, García-Colomo A, Cabrera-Álvarez J, Del Cerro-León A, Gómez-Ariza CJ, Santos A, et al. Individual alpha frequency tACS reduces static functional connectivity across the default mode network. Frontiers in Human Neuroscience. 2025; 19: 1534321. https://doi.org/10.3389/fnhum.2025.1534321
[55] Li Y, An S, Zhou T, Su C, Zhang S, Li C, et al. Triple-network analysis of Alzheimer's disease based on the energy landscape. Frontiers in Neuroscience. 2023; 17: 1171549. https://doi.org/10.3389/fnins.2023.1171549
[56] Xing L, Guo Z, Long Z. Energy landscape analysis of brain network dynamics in Alzheimer's disease. Frontiers in Aging Neuroscience. 2024; 16: 1375091. https://doi.org/10.3389/fnagi.2024.1375091
[57] Trufanov A, Markin K, Frunza D, Litvinenko I, Odinak M. Alterations in internetwork functional connectivity in patients with chronic migraine within the boundaries of the Triple Network Model. Neurology and Clinical Neuroscience. 2020; 8: 289–297.
[58] Payne LA, Seidman LC, Napadow V, Nickerson LD, Kumar P. Functional connectivity associations with menstrual pain characteristics in adolescents: an investigation of the triple network model. Pain. 2025; 166: 338–346. https://doi.org/10.1097/j.pain.0000000000003334

[59] Zhao R, Ye Z, Lv X, Li Z, Xiong X. Imaging Brain Networks: Insights into Mechanisms of Temporomandibular Disorders. Journal of Dental Research. 2025; 104: 380–388. https://doi.org/10.1177/00220345241302046
[60] Son JJ, Rice DL, Schantell M, Picci G, Okelberry HJ, Coutant AT, et al. Social pain is associated with altered developmental trajectories of connectivity among the triple network model of psychopathology. Social Cognitive and Affective Neuroscience. 2025; 20: nsaf037. https://doi.org/10.1093/scan/nsaf037
[61] Li X, Jia X, Liu Y, Bai G, Pan Y, Ji Q, et al. Brain dynamics in triple-network interactions and its relation to multiple cognitive impairments in mild traumatic brain injury. Cerebral Cortex (New York, N.Y. : 1991). 2023; 33: 6620–6632. https://doi.org/10.1093/cercor/bhac529
[62] Li F, Ren J, Lu L, Chen Y, Yin X. Changes in functional connectivity in patients with acute mild traumatic brain injury based on a triple-network model: a resting state functional MRI study. Chinese Journal of Behavioral Medicine and Brain Science. 2023; 231–237. (In Chinese)
[63] Liu H, Zhang G, Zheng H, Tan H, Zhuang J, Li W, et al. Dynamic Dysregulation of the Triple Network of the Brain in Mild Traumatic Brain Injury and Its Relationship With Cognitive Performance. Journal of Neurotrauma. 2024; 41: 879–886. https://doi.org/10.1089/neu.2022.0257
[64] Wang Y, Chen S, Xia X, Peng Y, Wu B. Altered functional connectivity and regional brain activity in a triple-network model in minimally conscious state and vegetative-state/unresponsive wakefulness syndrome patients: A resting-state functional magnetic resonance imaging study. Frontiers in Behavioral Neuroscience. 2022; 16: 1001519. https://doi.org/10.3389/fnbeh.2022.1001519
[65] Siste K, Pandelaki J, Miyata J, Oishi N, Tsurumi K, Fujiwara H, et al. Altered Resting-State Network in Adolescents with Problematic Internet Use. Journal of Clinical Medicine. 2022; 11: 5838. https://doi.org/10.3390/jcm11195838
[66] Shibata M, Tsurumi K, Kobayashi K, Yoshimura S, Spantios M, Oishi N, et al. Alterations of the default mode network, salience network, and frontoparietal network in non-problematic Internet use and their association with mood regulation: from an internet literacy perspective. Frontiers in Neuroscience. 2025; 19: 1599987. https://doi.org/10.3389/fnins.2025.1599987
[67] Aoki Y, Ishii R, Pascual-Marqui RD, Canuet L, Ikeda S, Hata M, et al. Detection of EEG-resting state independent networks by eLORETA-ICA method. Frontiers in Human Neuroscience. 2015; 9: 31. https://doi.org/10.3389/fnhum.2015.00031
[68] Pable H, Pham MD, Dehnavi MM, Chhabra R, D'Angiulli A. Neural self-organization during episodic encoding: deep recurrent effective connectivity from source-localized EEG. Frontiers in Psychology. 2026; 17: 1766795. https://doi.org/10.3389/fpsyg.2026.1766795
[69] Das A, Menon V. Electrophysiological dynamics of salience, default mode, and frontoparietal networks during episodic memory formation and recall revealed through multi-experiment iEEG replication. elife. 2024; 13: RP99018. https://doi.org/10.7554/eLife.99018
[70] Iyer A, Stanford W, Dayan E, Xavier RM. Salience network segregation and symptom profiles in psychosis risk subgroups among youth and early adults. Schizophrenia (Heidelberg, Germany). 2025; 11: 142. https://doi.org/10.1038/s41537-025-00687-x
[71] Iordan AD, Ploutz-Snyder R, Ghosh B, Rahman-Filipiak A, Koeppe R, Peltier S, et al. Salience network segregation mediates the effect of tau pathology on mild behavioral impairment. Alzheimer's & Dementia : the Journal of the Alzheimer's Association. 2024; 20: 7675–7685. https://doi.org/10.1002/alz.14229
[72] Sarkis-Onofre R, Catalá-López F, Aromataris E, Lockwood C. How to properly use the PRISMA Statement. Systematic Reviews. 2021; 10: 117. https://doi.org/10.1186/s13643-021-01671-z
[73] Landauer TK, Foltz PW, Laham D. An introduction to latent semantic analysis. Discourse Processes. 1998; 25: 259–284.
[74] Blei DM, Ng AY, Jordan MI. Latent dirichlet allocation. Journal of Machine Learning Research. 2003; 3: 993–1022.
[75] Zhu C, Fu Z, Chen L, Yu F, Zhang J, Zhang Y, et al. Multimodality connectome-based predictive modeling of individualized compulsions in obsessive-compulsive disorder. Journal of Affective Disorders. 2022; 311: 595–603. https://doi.org/10.1016/j.jad.2022.05.120
[76] Sarraf S, Sun J. Advances in functional brain imaging: a comprehensive survey for engineers and physical scientists. International Journal of Advanced Research. 2016; 4: 640–660.
[77] Finn ES, Poldrack RA, Shine JM. Functional neuroimaging as a catalyst for integrated neuroscience. Nature. 2023; 623: 263–273. https://doi.org/10.1038/s41586-023-06670-9
[78] Turner BO, Paul EJ, Miller MB, Barbey AK. Small sample sizes reduce the replicability of task-based fMRI studies. Communications Biology. 2018; 1: 62. https://doi.org/10.1038/s42003-018-0073-z
[79] Marek S, Tervo-Clemmens B, Calabro FJ, Montez DF, Kay BP, Hatoum AS, et al. Reproducible brain-wide association studies require thousands of individuals. Nature. 2022; 603: 654–660. https://doi.org/10.1038/s41586-022-04492-9
[80] Ooi LQR, Orban C, Zhang S, Nichols TE, Tan TWK, Kong R, et al. Longer scans boost prediction and cut costs in brain-wide association studies. Nature. 2025; 644: 731–740. https://doi.org/10.1038/s41586-025-09250-1
[81] Logothetis NK. What we can do and what we cannot do with fMRI. Nature. 2008; 453: 869–878. https://doi.org/10.1038/nature06976
[82] Townsend DW. Physical principles and technology of clinical PET imaging. Annals of the Academy of Medicine, Singapore. 2004; 33: 133–145.
[83] Agdeppa ED, Spilker ME. A review of imaging agent development. The AAPS Journal. 2009; 11: 286–299. https://doi.org/10.1208/s12248-009-9104-5
[84] Grech R, Cassar T, Muscat J, Camilleri KP, Fabri SG, Zervakis M, et al. Review on solving the inverse problem in EEG source analysis. Journal of Neuroengineering and Rehabilitation. 2008; 5: 25. https://doi.org/10.1186/1743-0003-5-25
[85] Li Y, Wang Y, Xu F, Jiang T, Wang X. Combination of magnetoencephalographic and clinical features to identify atypical self-limited epilepsy with centrotemporal spikes. Epilepsy & Behavior : E&B. 2024; 161: 110095. https://doi.org/10.1016/j.yebeh.2024.110095
[86] Gündüz E, Demirbilek V, Korkmaz B. Benign rolandic epilepsy: neuropsychological findings. Seizure. 1999; 8: 246–249. https://doi.org/10.1053/seiz.1999.0293
[87] Lopes da Silva F. EEG and MEG: relevance to neuroscience. Neuron. 2013; 80: 1112–1128. https://doi.org/10.1016/j.neuron.2013.10.017
[88] Zhang YD, Dong Z, Wang SH, Yu X, Yao X, Zhou Q, et al. Advances in multimodal data fusion in neuroimaging: Overview, challenges, and novel orientation. An International Journal on Information Fusion. 2020; 64: 149–187. https://doi.org/10.1016/j.inffus.2020.07.006
[89] Jirsaraie RJ, Gorelik AJ, Gatavins MM, Engemann DA, Bogdan R, Barch DM, et al. A systematic review of multimodal brain age studies: Uncovering a divergence between model accuracy and utility. Patterns (New York, N.Y.). 2023; 4: 100712. https://doi.org/10.1016/j.patter.2023.100712
[90] Banihashemi L, Lv J, Wu M, Zhan L. Editorial: Current ad-

vances in multimodal human brain imaging and analysis across the lifespan: From mapping to state prediction. Frontiers in Neuroscience. 2023; 17: 1153035. https://doi.org/10.3389/fnins.2023.1153035

[91] Horwitz B, Poeppel D. How can EEG/MEG and fMRI/PET data be combined? Human Brain Mapping. 2002; 17: 1–3. https://doi.org/10.1002/hbm.10057

[92] Jorge J, van der Zwaag W, Figueiredo P. EEG-fMRI integration for the study of human brain function. NeuroImage. 2014; 102 Pt 1: 24–34. https://doi.org/10.1016/j.neuroimage.2013.05.114

[93] Chang C, Chen JE. Multimodal EEG-fMRI: advancing insight into large-scale human brain dynamics. Current Opinion in Biomedical Engineering. 2021; 18: 100279. https://doi.org/10.1016/j.cobme.2021.100279

[94] Thatcher RW. Coherence, phase differences, phase shift, and phase lock in EEG/ERP analyses. Developmental Neuropsychology. 2012; 37: 476–496. https://doi.org/10.1080/87565641.2011.619241

[95] Schmidt BT, Ghuman AS, Huppert TJ. Whole brain functional connectivity using phase locking measures of resting state magnetoencephalography. Frontiers in Neuroscience. 2014; 8: 141. https://doi.org/10.3389/fnins.2014.00141

[96] Jann K, Dierks T, Boesch C, Kottlow M, Strik W, Koenig T. BOLD correlates of EEG alpha phase-locking and the fMRI default mode network. NeuroImage. 2009; 45: 903–916. https://doi.org/10.1016/j.neuroimage.2009.01.001

[97] Michels L, Riese F, Meyer R, Kälin AM, Leh SE, Unschuld PG, et al. EEG-fMRI Signal Coupling Is Modulated in Subjects With Mild Cognitive Impairment and Amyloid Deposition. Frontiers in Aging Neuroscience. 2021; 13: 631172. https://doi.org/10.3389/fnagi.2021.631172

[98] Michel CM, He B. EEG source localization. Handbook of Clinical Neurology. 2019; 160: 85–101. https://doi.org/10.1016/B978-0-444-64032-1.00006-0

[99] Schoffelen JM, Gross J. Source connectivity analysis with MEG and EEG. Human Brain Mapping. 2009; 30: 1857–1865. https://doi.org/10.1002/hbm.20745

[100] Mosher JC, Leahy RM, Lewis PS. EEG and MEG: forward solutions for inverse methods. IEEE Transactions on Bio-medical Engineering. 1999; 46: 245–259. https://doi.org/10.1109/10.748978

[101] Hallez H, Vanrumste B, Grech R, Muscat J, De Clercq W, Vergult A, et al. Review on solving the forward problem in EEG source analysis. Journal of Neuroengineering and Rehabilitation. 2007; 4: 46. https://doi.org/10.1186/1743-0003-4-46

[102] Michel CM, Brunet D. EEG Source Imaging: A Practical Review of the Analysis Steps. Frontiers in Neurology. 2019; 10: 325. https://doi.org/10.3389/fneur.2019.00325

[103] Lahtinen J, Koulouri A. Overview of Bayesian Solvers in EEG Distributed Source Models: Prior Selection, Algorithmic Implementation, and Depth Bias Reduction. arXiv preprint arXiv:2604.05913. 2026. (preprint)

[104] Hauk O. Keep it simple: a case for using classical minimum norm estimation in the analysis of EEG and MEG data. NeuroImage. 2004; 21: 1612–1621. https://doi.org/10.1016/j.neuroimage.2003.12.018

[105] Jonmohamadi Y, Poudel G, Innes C, Weiss D, Krueger R, Jones R. Comparison of beamformers for EEG source signal reconstruction. Biomedical Signal Processing and Control. 2014; 14: 175–188.

[106] Wipf D, Nagarajan S. A unified Bayesian framework for MEG/EEG source imaging. NeuroImage. 2009; 44: 947–966. https://doi.org/10.1016/j.neuroimage.2008.02.059

[107] Feng Z, Guan C, Sun Y. Block-Champagne: A Novel Bayesian Framework for Imaging Extended E/MEG Source. IEEE Transactions on Medical Imaging. 2026; 45: 1986–2000. https://doi.org/10.1109/TMI.2025.3642620

[108] Mannepalli T, Routray A. Sparse algorithms for EEG source localization. Medical & Biological Engineering & Computing. 2021; 59: 2325–2352. https://doi.org/10.1007/s11517-021-02444-5

[109] Basri SMM, Al-Nashash H, Mir H. Inverse problem for M/EEG source localization: a review. IEEE Sensors Journal. 2024; 25: 2103–2124.

[110] Dattola S, Morabito FC, Mammone N, La Foresta F. Findings about LORETA applied to high-density EEG—A review. Electronics. 2020; 9: 660.

[111] Kim J, Wozniak JR, Mueller BA, Pan W. Testing group differences in brain functional connectivity: using correlations or partial correlations? Brain Connectivity. 2015; 5: 214–231.

[112] Peterson KL, Sanchez-Romero R, Mill RD, Cole MW. Regularized partial correlation provides reliable functional connectivity estimates while correcting for widespread confounding. Imaging Neuroscience (Cambridge, Mass.). 2025; 3: IMAG.a.162. https://doi.org/10.1162/IMAG.a.162

[113] Hutchison RM, Womelsdorf T, Allen EA, Bandettini PA, Calhoun VD, Corbetta M, et al. Dynamic functional connectivity: promise, issues, and interpretations. NeuroImage. 2013; 80: 360–378. https://doi.org/10.1016/j.neuroimage.2013.05.079

[114] Gonzalez-Castillo J, Bandettini PA. Task-based dynamic functional connectivity: Recent findings and open questions. NeuroImage. 2018; 180: 526–533. https://doi.org/10.1016/j.neuroimage.2017.08.006

[115] Lurie DJ, Kessler D, Bassett DS, Betzel RF, Breakspear M, Kheilholz S, et al. Questions and controversies in the study of time-varying functional connectivity in resting fMRI. Network Neuroscience (Cambridge, Mass.). 2020; 4: 30–69. https://doi.org/10.1162/netn_a_00116

[116] Vidaurre D. Dynamic functional connectivity: Why the controversy? Imaging Neuroscience (Cambridge, Mass.). 2024; 2: imag–imag–2–00363. https://doi.org/10.1162/imag_a_00363

[117] Laumann TO, Snyder AZ, Gratton C. Challenges in the measurement and interpretation of dynamic functional connectivity. Imaging Neuroscience (Cambridge, Mass.). 2024; 2: imag–imag–2–00366. https://doi.org/10.1162/imag_a_00366

[118] Friston KJ. Functional and effective connectivity: a review. Brain Connectivity. 2011; 1: 13–36. https://doi.org/10.1089/brain.2011.0008

[119] Shojaie A, Fox EB. Granger Causality: A Review and Recent Advances. Annual Review of Statistics and its Application. 2022; 9: 289–319. https://doi.org/10.1146/annurev-statistics-040120-010930

[120] Friston K, Moran R, Seth AK. Analysing connectivity with Granger causality and dynamic causal modelling. Current Opinion in Neurobiology. 2013; 23: 172–178. https://doi.org/10.1016/j.conb.2012.11.010

[121] Bajaj S, Adhikari BM, Friston KJ, Dhamala M. Bridging the Gap: Dynamic Causal Modeling and Granger Causality Analysis of Resting State Functional Magnetic Resonance Imaging. Brain Connectivity. 2016; 6: 652–661. https://doi.org/10.1089/brain.2016.0422

[122] Roland PE, Graufelds CJ, W Hlin J, Ingelman L, Andersson M, Ledberg A, et al. Human brain atlas: For high-resolution functional and anatomical mapping. Human Brain Mapping. 1994; 1: 173–184. https://doi.org/10.1002/hbm.460010303

[123] Bohland JW, Bokil H, Allen CB, Mitra PP. The brain atlas concordance problem: quantitative comparison of anatomical parcellations. PloS One. 2009; 4: e7200. https://doi.org/10.1371/journal.pone.0007200

[124] Evans AC, Janke AL, Collins DL, Baillet S. Brain templates and atlases. NeuroImage. 2012; 62: 911–922. https://doi.org/10.1016/j.neuroimage.2012.01.024

[125] Mandal PK, Mahajan R, Dinov ID. Structural brain atlases: design, rationale, and applications in normal and pathological cohorts. Journal of Alzheimer's Disease : JAD. 2012; 31 Suppl 3: S169–S188. https://doi.org/10.3233/JAD-2012-120412
[126] Fan L, Li H, Zhuo J, Zhang Y, Wang J, Chen L, et al. The Human Brainnetome Atlas: A New Brain Atlas Based on Connectional Architecture. Cerebral Cortex (New York, N.Y. : 1991). 2016; 26: 3508–3526. https://doi.org/10.1093/cercor/bhw157
[127] Fischl B, Salat DH, Busa E, Albert M, Dieterich M, Haselgrove C, et al. Whole brain segmentation: automated labeling of neuroanatomical structures in the human brain. Neuron. 2002; 33: 341–355. https://doi.org/10.1016/s0896-6273(02)00569-x
[128] D'Angelo E, Jirsa V. The quest for multiscale brain modeling. Trends in Neurosciences. 2022; 45: 777–790. https://doi.org/10.1016/j.tins.2022.06.007
[129] Dickie DA, Shenkin SD, Anblagan D, Lee J, Blesa Cabez M, Rodriguez D, et al. Whole Brain Magnetic Resonance Image Atlases: A Systematic Review of Existing Atlases and Caveats for Use in Population Imaging. Frontiers in Neuroinformatics. 2017; 11: 1. https://doi.org/10.3389/fninf.2017.00001
[130] Lawrence RM, Bridgeford EW, Myers PE, Arvapalli GC, Ramachandran SC, Pisner DA, et al. Standardizing human brain parcellations. Scientific Data. 2021; 8: 78. https://doi.org/10.1038/s41597-021-00849-3
[131] Nowinski WL. Evolution of Human Brain Atlases in Terms of Content, Applications, Functionality, and Availability. Neuroinformatics. 2021; 19: 1–22. https://doi.org/10.1007/s12021-020-09481-9
[132] Pham MD, D'Angiulli A, Dehnavi MM, Chhabra R. From Brain Models to Robotic Embodied Cognition: How Does Biological Plausibility Inform Neuromorphic Systems? Brain Sciences. 2023; 13: 1316. https://doi.org/10.3390/brainsci13091316
[133] Mazziotta J, Toga A, Evans A, Fox P, Lancaster J, Zilles K, et al. A four-dimensional probabilistic atlas of the human brain. Journal of the American Medical Informatics Association : JAMIA. 2001; 8: 401–430. https://doi.org/10.1136/jamia.2001.0080401
[134] Yeo BTT, Krienen FM, Sepulcre J, Sabuncu MR, Lashkari D, Hollinshead M, et al. The organization of the human cerebral cortex estimated by intrinsic functional connectivity. Journal of Neurophysiology. 2011; 106: 1125–1165. https://doi.org/10.1152/jn.00338.2011
[135] Alexander B, Loh WY, Matthews LG, Murray AL, Adamson C, Beare R, et al. Desikan-Killiany-Tourville Atlas Compatible Version of M-CRIB Neonatal Parcellated Whole Brain Atlas: The M-CRIB 2.0. Frontiers in Neuroscience. 2019; 13: 34. https://doi.org/10.3389/fnins.2019.00034
[136] McGrath H, Zaveri HP, Collins E, Jafar T, Chishti O, Obaid S, et al. High-resolution cortical parcellation based on conserved brain landmarks for localization of multimodal data to the nearest centimeter. Scientific Reports. 2022; 12: 18778. https://doi.org/10.1038/s41598-022-21543-3
[137] Zhernovaia M, Dadar M, Mahmoud S, Zeighami Y, Maranzano J. The PaleoArchiNeo (PAN) human brain atlas: A dataset on a standard neuroanatomical MRI template following a phylogenetic approach. Data in Brief. 2022; 41: 107863. https://doi.org/10.1016/j.dib.2022.107863
[138] Gorgolewski KJ, Varoquaux G, Rivera G, Schwarz Y, Ghosh SS, Maumet C, et al. NeuroVault.org: a web-based repository for collecting and sharing unthresholded statistical maps of the human brain. Frontiers in Neuroinformatics. 2015; 9: 8. https://doi.org/10.3389/fninf.2015.00008
[139] Fischl B. FreeSurfer. NeuroImage. 2012; 62: 774–781. https://doi.org/10.1016/j.neuroimage.2012.01.021
[140] Manjón JV, Coupé P. volBrain: An Online MRI Brain Volumetry System. Frontiers in Neuroinformatics. 2016; 10: 30. https://doi.org/10.3389/fninf.2016.00030
[141] Emekli E, Demirel BC, Emekli E, Toprak U. Consistency and differences of cortical thickness measurements among FreeSurfer, FastSurfer, BrainVolume, and volBrain softwares. In: 25th National Anatomy Congress. 2025.
[142] Fox MD, Snyder AZ, Vincent JL, Corbetta M, Van Essen DC, Raichle ME. The human brain is intrinsically organized into dynamic, anticorrelated functional networks. Proceedings of the National Academy of Sciences of the United States of America. 2005; 102: 9673–9678. https://doi.org/10.1073/pnas.0504136102
[143] Müller VI, Cieslik EC, Laird AR, Fox PT, Radua J, Mataix-Cols D, et al. Ten simple rules for neuroimaging meta-analysis. Neuroscience and Biobehavioral Reviews. 2018; 84: 151–161. https://doi.org/10.1016/j.neubiorev.2017.11.012
[144] Parvizi J, Kastner S. Promises and limitations of human intracranial electroencephalography. Nature Neuroscience. 2018; 21: 474–483. https://doi.org/10.1038/s41593-018-0108-2
[145] Andrews-Hanna JR, Smallwood J, Spreng RN. The default network and self-generated thought: component processes, dynamic control, and clinical relevance. Annals of the New York Academy of Sciences. 2014; 1316: 29–52. https://doi.org/10.1111/nyas.12360
[146] Christoff K, Gordon AM, Smallwood J, Smith R, Schooler JW. Experience sampling during fMRI reveals default network and executive system contributions to mind wandering. Proceedings of the National Academy of Sciences of the United States of America. 2009; 106: 8719–8724. https://doi.org/10.1073/pnas.0900234106
[147] Girn M, Mills C, Laycock E, Ellamil M, Ward L, Christoff K. Neural dynamics of spontaneous thought: an electroencephalographic study. International Conference on Augmented Cognition (pp. 28–44). Springer: Cham. 2017.
[148] Christian BM, Miles LK, Parkinson C, Macrae CN. Visual perspective and the characteristics of mind wandering. Frontiers in Psychology. 2013; 4: 699. https://doi.org/10.3389/fpsyg.2013.00699
[149] Choi H, Geden M, Feng J. More visual mind wandering occurrence during visual task performance: Modality of the concurrent task affects how the mind wanders. PloS One. 2017; 12: e0189667. https://doi.org/10.1371/journal.pone.0189667
[150] Wens V, Bourguignon M, Vander Ghinst M, Mary A, Marty B, Coquelet N, et al. Synchrony, metastability, dynamic integration, and competition in the spontaneous functional connectivity of the human brain. NeuroImage. 2019; 199: 313–324. https://doi.org/10.1016/j.neuroimage.2019.05.081
[151] Vatansever D, Menon DK, Manktelow AE, Sahakian BJ, Stamatakis EA. Default Mode Dynamics for Global Functional Integration. The Journal of Neuroscience : the Official Journal of the Society for Neuroscience. 2015; 35: 15254–15262. https://doi.org/10.1523/JNEUROSCI.2135-15.2015
[152] Hancock F, Rosas FE, Luppi AI, Zhang M, Mediano PAM, Cabral J, et al. Metastability demystified - the foundational past, the pragmatic present and the promising future. Nature Reviews. Neuroscience. 2025; 26: 82–100. https://doi.org/10.1038/s41583-024-00883-1
[153] Wijaya MT, Mabel-Kenzie STST, Ouyang G, Lee TMC. Metastability in the wild: A scoping review of empirical neuroimaging studies in humans. Neuroscience and Biobehavioral Reviews. 2025; 172: 106106. https://doi.org/10.1016/j.neubiorev.2025.106106
[154] Dixon ML, De La Vega A, Mills C, Andrews-Hanna J, Spreng RN, Cole MW, et al. Heterogeneity within the frontoparietal control network and its relationship to the default and dorsal attention networks. Proceedings of the National Academy of

Sciences of the United States of America. 2018; 115: E1598–E1607. https://doi.org/10.1073/pnas.1715766115
[155] Geng H, Xu P, Aleman A, Qin S, Luo YJ. Dynamic Organization of Large-scale Functional Brain Networks Supports Interactions Between Emotion and Executive Control. Neuroscience Bulletin. 2024; 40: 981–991. https://doi.org/10.1007/s12264-023-01168-w
[156] Witt ST, van Ettinger-Veenstra H, Salo T, Riedel MC, Laird AR. What Executive Function Network is that? An Image-Based Meta-Analysis of Network Labels. Brain Topography. 2021; 34: 598–607. https://doi.org/10.1007/s10548-021-00847-z
[157] Laird AR, Eickhoff SB, Li K, Robin DA, Glahn DC, Fox PT. Investigating the functional heterogeneity of the default mode network using coordinate-based meta-analytic modeling. The Journal of Neuroscience : the Official Journal of the Society for Neuroscience. 2009; 29: 14496–14505. https://doi.org/10.1523/JNEUROSCI.4004-09.2009
[158] Wen T, Mitchell DJ, Duncan J. The Functional Convergence and Heterogeneity of Social, Episodic, and Self-Referential Thought in the Default Mode Network. Cerebral Cortex (New York, N.Y. : 1991). 2020; 30: 5915–5929. https://doi.org/10.1093/cercor/bhaa166
[159] Andre Z, Kalina CH. Default heterogeneity: from a singular construct to multiple default network(s). Current Opinion in Behavioral Sciences. 2026; 68: 101636. https://doi.org/10.1016/j.cobeha.2026.101636
[160] Hegarty AK, Yani MS, Albishi A, Michener LA, Kutch JJ. Salience network functional connectivity is spatially heterogeneous across sensorimotor cortex in healthy humans. NeuroImage. 2020; 221: 117177. https://doi.org/10.1016/j.neuroimage.2020.117177
[161] Guo X, Zhai G, Liu J, Zhang X, Zhang T, Cui D, et al. Heterogeneity of dynamic synergetic configurations of salience network in children with autism spectrum disorder. Autism Research : Official Journal of the International Society for Autism Research. 2023; 16: 2275–2290. https://doi.org/10.1002/aur.3037
[162] Guo X, Zhang X, Liu J, Zhai G, Zhang T, Zhou R, et al. Resolving heterogeneity in dynamics of synchronization stability within the salience network in autism spectrum disorder. Progress in Neuro-psychopharmacology & Biological Psychiatry. 2024; 131: 110956. https://doi.org/10.1016/j.pnpbp.2024.110956
[163] Manoliu A, Meng C, Brandl F, Doll A, Tahmasian M, Scherr M, et al. Insular dysfunction within the salience network is associated with severity of symptoms and aberrant inter-network connectivity in major depressive disorder. Frontiers in Human Neuroscience. 2014; 7: 930. https://doi.org/10.3389/fnhum.2013.00930
[164] Li X, Kass G, Wiers CE, Shi Z. The Brain Salience Network at the Intersection of Pain and Substance use Disorders: Insights from Functional Neuroimaging Research. Current Addiction Reports. 2024; 11: 797–808. https://doi.org/10.1007/s40429-024-00593-9
[165] Kao TC, Hennequin G. Neuroscience out of control: control-theoretic perspectives on neural circuit dynamics. Current Opinion in Neurobiology. 2019; 58: 122–129. https://doi.org/10.1016/j.conb.2019.09.001
[166] Madhav MS, Cowan NJ. The synergy between neuroscience and control theory: the nervous system as inspiration for hard control challenges. Annual Review of Control, Robotics, and Autonomous Systems. 2020; 3: 243–267.
[167] Tin C, Poon CS. Internal models in sensorimotor integration: perspectives from adaptive control theory. Journal of Neural Engineering. 2005; 2: S147–S163. https://doi.org/10.1088/1741-2560/2/3/S01
[168] Scott SH. Optimal feedback control and the neural basis of volitional motor control. Nature Reviews. Neuroscience. 2004; 5: 532–546. https://doi.org/10.1038/nrn1427
[169] Guenther FH. Neural control of speech. Mit Press: Cambridge, Massachusetts London, England. 2016.
[170] Todorov E. Optimal control theory. Bayesian Brain: Probabilistic Approaches to Neural Coding. 2006: 268–298.
[171] Eliasmith C, Anderson CH. Neural engineering: Computation, representation, and dynamics in neurobiological systems. MIT press: Cambridge, Massachusetts London, England. 2003.
[172] Schiff SJ. Neural control engineering: the emerging intersection between control theory and neuroscience. MIT press: Cambridge, Massachusetts London, England. 2011.
[173] Kudithipudi D, Schuman C, Vineyard CM, Pandit T, Merkel C, Kubendran R, et al. Neuromorphic computing at scale. Nature. 2025; 637: 801–812. https://doi.org/10.1038/s41586-024-08253-8
[174] Medaglia JD, Pasqualetti F, Hamilton RH, Thompson-Schill SL, Bassett DS. Brain and cognitive reserve: Translation via network control theory. Neuroscience and Biobehavioral Reviews. 2017; 75: 53–64. https://doi.org/10.1016/j.neubiorev.2017.01.016
[175] Lynn CW, Bassett DS. The physics of brain network structure, function and control. Nature Reviews Physics. 2019; 1: 318–332.
[176] Wu Z, Huang L, Wang M, He X. Development of the brain network control theory and its implications. Psychoradiology. 2024; 4: kkae028. https://doi.org/10.1093/psyrad/kkae028
[177] Lenglet C, Prados E, Pons JP, Deriche R, Faugeras O. Brain connectivity mapping using Riemannian geometry, control theory, and PDEs. SIAM Journal on Imaging Sciences. 2009; 2: 285–322.
[178] Do Carmo MP, Flaherty Francis J. Riemannian geometry. vol. 393. Springer: Boston. 1992.
[179] Tibermacine IE, Russo S, Tibermacine A, Rabehi A, Nail B, Kadri K, et al. Riemannian geometry-based eeg approaches: A literature review. arXiv preprint arXiv: 2407. 20250. 2024. (preprint)
[180] Yger F, Berar M, Lotte F. Riemannian Approaches in Brain-Computer Interfaces: A Review. IEEE Transactions on Neural Systems and Rehabilitation Engineering : a Publication of the IEEE Engineering in Medicine and Biology Society. 2017; 25: 1753–1762. https://doi.org/10.1109/TNSRE.2016.2627016
[181] Congedo M, Barachant A, Bhatia R. Riemannian geometry for EEG-based brain-computer interfaces; a primer and a review. Brain-Computer Interfaces. 2017; 4: 155–174.
[182] Paillard J, Hipp JF, Engemann DA. GREEN: A lightweight architecture using learnable wavelets and Riemannian geometry for biomarker exploration with EEG signals. Patterns (New York, N.Y.). 2025; 6: 101182. https://doi.org/10.1016/j.patter.2025.101182
[183] Arsigny V, Fillard P, Pennec X, Ayache N. Log-Euclidean metrics for fast and simple calculus on diffusion tensors. Magnetic Resonance in Medicine. 2006; 56: 411–421. https://doi.org/10.1002/mrm.20965
[184] Fletcher PT, Joshi S. Principal geodesic analysis on symmetric spaces: Statistics of diffusion tensors. International Workshop on Mathematical Methods in Medical and Biomedical Image Analysis (pp. 87–98). Springer: Berlin, Heidelberg. 2004.
[185] You K, Park HJ. Re-visiting Riemannian geometry of symmetric positive definite matrices for the analysis of functional connectivity. NeuroImage. 2021; 225: 117464. https://doi.org/10.1016/j.neuroimage.2020.117464
[186] You K, Park HJ. Geometric learning of functional brain network on the correlation manifold. Scientific Reports. 2022; 12:

17752. https://doi.org/10.1038/s41598-022-21376-0
[187] Mitchell-Heggs R, Prado S, Gava GP, Go MA, Schultz SR. Neural manifold analysis of brain circuit dynamics in health and disease. Journal of Computational Neuroscience. 2023; 51: 1–21. https://doi.org/10.1007/s10827-022-00839-3
[188] Huang Z, Van Gool L. A riemannian network for spd matrix learning. In Proceedings of the AAAI conference on artificial intelligence. Hilton San Francisco Union Square. AAAI Press. 2017.
[189] Perich MG, Narain D, Gallego JA. A neural manifold view of the brain. Nature Neuroscience. 2025; 28: 1582–1597. https://doi.org/10.1038/s41593-025-02031-z
[190] Dan T, Huang Z, Cai H, Laurienti PJ, Wu G. Learning Brain Dynamics of Evolving Manifold Functional MRI Data Using Geometric-Attention Neural Network. IEEE Transactions on Medical Imaging. 2022; 41: 2752–2763. https://doi.org/10.1109/TMI.2022.3169640
[191] Qiu A, Lee A, Tan M, Chung MK. Manifold learning on brain functional networks in aging. Medical Image Analysis. 2015; 20: 52–60. https://doi.org/10.1016/j.media.2014.10.006
[192] Simeon G, Piella G, Camara O, Pareto D. Riemannian Geometry of Functional Connectivity Matrices for Multi-Site Attention-Deficit/Hyperactivity Disorder Data Harmonization. Frontiers in Neuroinformatics. 2022; 16: 769274. https://doi.org/10.3389/fninf.2022.769274
[193] Pezon L, Schmutz V, Gerstner W. Linking neural manifolds to circuit structure in recurrent networks. Neuron. 2026; 114: 1682–1694.e21. https://doi.org/10.1016/j.neuron.2025.12.047
[194] Langdon C, Genkin M, Engel TA. A unifying perspective on neural manifolds and circuits for cognition. Nature Reviews. Neuroscience. 2023; 24: 363–377. https://doi.org/10.1038/s41583-023-00693-x
[195] Gosztolai A, Peach RL, Arnaudon A, Barahona M, Vandergheynst P. MARBLE: interpretable representations of neural population dynamics using geometric deep learning. Nature Methods. 2025; 22: 612–620. https://doi.org/10.1038/s41592-024-02582-2
[196] Gallego JA, Perich MG, Miller LE, Solla SA. Neural Manifolds for the Control of Movement. Neuron. 2017; 94: 978–984. https://doi.org/10.1016/j.neuron.2017.05.025
[197] Gallego JA, Perich MG, Naufel SN, Ethier C, Solla SA, Miller LE. Cortical population activity within a preserved neural manifold underlies multiple motor behaviors. Nature Communications. 2018; 9: 4233. https://doi.org/10.1038/s41467-018-06560-z
[198] Ma H, Jiang L, Liu T, Liu J. From sensory to perceptual manifolds: The twist of neural geometry. Science Advances. 2025; 11: eadv0431. https://doi.org/10.1126/sciadv.adv0431
[199] Rué-Queralt J, Stevner A, Tagliazucchi E, Laufs H, Kringelbach ML, Deco G, et al. Decoding brain states on the intrinsic manifold of human brain dynamics across wakefulness and sleep. Communications Biology. 2021; 4: 854. https://doi.org/10.1038/s42003-021-02369-7
[200] Wakhloo AJ, Slatton W, Chung S. Neural population geometry and optimal coding of tasks with shared latent structure. Nature Neuroscience. 2026; 29: 682–692. https://doi.org/10.1038/s41593-025-02183-y
[201] Ebin DG. The manifold of Riemannian metrics. Proceedings of Symposia in Pure Mathematics. 1970; 15: 11–40.
[202] Ju C, Kobler RJ, Collas A, Kawanabe M, Guan C, Thirion B. SPD Learning for Covariance-Based Neuroimaging Analysis: Perspectives, Methods, and Challenges. arXiv preprint arXiv: 2504.18882. 2025. (preprint)
[203] Yamin A, Dayan M, Squarcina L, Brambilla P, Murino V, Diwadkar V, et al. Analysis of dynamic brain connectivity through geodesic clustering. International conference on image analysis and processing (pp. 640–648). Springer: Cham. 2019.
[204] Abbas K, Liu M, Venkatesh M, Amico E, Kaplan AD, Ventresca M, et al. Geodesic Distance on Optimally Regularized Functional Connectomes Uncovers Individual Fingerprints. Brain Connectivity. 2021; 11: 333–348. https://doi.org/10.1089/brain.2020.0881
[205] Slavakis K, Salsabilian S, Wack DS, Muldoon SF, Baidoo-Williams HE, Vettel JM, et al. Clustering brain-network time series by Riemannian geometry. IEEE Transactions on Signal and Information Processing over Networks. 2017; 4: 519–533.
[206] Zhang M, Fletcher T. Probabilistic principal geodesic analysis. Advances in Neural Information Processing Systems. 2013; 26.
[207] Pennec X. Intrinsic statistics on Riemannian manifolds: Basic tools for geometric measurements. Journal of Mathematical Imaging and Vision. 2006; 25: 127–154.
[208] Brunton SL, Proctor JL, Kutz JN. Discovering governing equations from data by sparse identification of nonlinear dynamical systems. Proceedings of the National Academy of Sciences of the United States of America. 2016; 113: 3932–3937. https://doi.org/10.1073/pnas.1517384113
[209] Koppe G, Toutounji H, Kirsch P, Lis S, Durstewitz D. Identifying nonlinear dynamical systems via generative recurrent neural networks with applications to fMRI. PLoS Computational Biology. 2019; 15: e1007263. https://doi.org/10.1371/journal.pcbi.1007263
[210] Klindt D, Ecker AS, Euler T, Bethge M. Neural system identification for large populations separating "what" and "where". Advances in Neural Information Processing Systems. 2017; 30.
[211] Han Y, Poggio TA, Cheung B. System identification of neural systems: If we got it right, would we know? In International Conference on Machine Learning (pp. 12430–12444). PMLR. 2023.
[212] Wilson RC, Collins AG. Ten simple rules for the computational modeling of behavioral data. elife. 2019; 8: e49547. https://doi.org/10.7554/eLife.49547
[213] Scheinost D, Noble S, Horien C, Greene AS, Lake EM, Salehi M, et al. Ten simple rules for predictive modeling of individual differences in neuroimaging. NeuroImage. 2019; 193: 35–45. https://doi.org/10.1016/j.neuroimage.2019.02.057